Grafting of the peppermint essential oil to a chemically treated Ti6Al4V alloy to counteract the bacterial adhesion

Elsevier Editorial System(tm) for Surface and Coatings Technology

Manuscript Draft

Manuscript Number: SURFCOAT-D-19-02316R1

Title: Grafting of peppermint essential oil to chemically treated Ti6Al4V alloy to counteract bacterial adhesion

Article Type: Full Length Article

Keywords: titanium; essential oils; coating; functionalization; antibacterial effect

Corresponding Author: Dr. Silvia Spriano, PhD

Corresponding Author's Institution: Politecnico di Torino

First Author: Martina Cazzola

Order of Authors: Martina Cazzola; Sara Ferraris; Valeria Allizond; Cinzia Bertea; Chiara Novara; Andrea Cochis; Francesco Geobaldo; Alessandro Bistolfi; Annamaria Cuffini; Lia Rimondini; Giuliana Banche; Silvia Spriano, PhD

Abstract: Essential oils are effective as alternative biocide molecules, but they are currently not used against bacterial contamination of surfaces for biomedical, industrial or everyday life applications.
In this work, the grafting of peppermint oil to a chemically-treated titanium alloy is explored as a coating or through functionalization (soaking in an ethanol solution of the oil); a procedure for a proper characterization of this type of materials is here suggested.
A homogeneous and continuous coating is obtained by polymerization of the oil on the titanium surface, as shown by fluorescence observation. It contains a prevalence of oxygenated compounds (gas-chromatographic, XPS and FTIR analysis), has a hydrophobic behavior (contact angle test and zeta potential titration) and shows strong adhesion to the substrate (tape test).
On the functionalized samples, the presence of non-oxygenated grafted compounds was detected (gas-chromatographic, XPS analysis) without the formation of a coating (fluorescent observation). The characteristics of the substrate combined to the selected functionalization procedure are selective towards grafting of specific compounds even if they are minority fractions in the source peppermint oil. The coating has a bacteriostatic effect on adherent bacteria, which is lower on the functionalized samples.

1. Introduction

Bacterial contamination of surfaces is a relevant issue not only for medical and biomedical devices, but also in industrial processes and everyday life. Moreover, the incidence of bacterial drug resistance is increasing and side effects and toxicity limit the long-term use of antibiotics: alternative ways to fight or prevent infections are a high medical need and several surface modifications techniques and coatings for antibacterial applications were recently developed [1].

Essential Oils (EOs) and their components have been shown to have antibacterial effects against Gram-positive and Gram-negative bacteria and they may respond to the need of novel alternative biocide molecules [2]. The EO hydrophobicity disrupts the bacteria wall [3] and increases its permeability interfering with cellular processes like energy balance, solute transport and regulation of metabolism. After degradation of the cell wall, EOs are able to damage the cytoplasmic membrane, to coagulate the cytoplasm, to denature proteins, to reduce ATP synthesis, proton motive force and membrane potential [4]. Interacting with the membrane, EOs can also reduce the production of toxins by bacteria both disrupting the phospholipid bilayer and limiting transmembrane transport and release. Moreover, the protein synthesis can be modified by these molecules, as it was demonstrated for p-cymene and carvacrol, two EO common components, able to induce the synthesis of heat shock proteins in bacteria. EOs modify the internal pH of bacterial cells interfering in cell homeostasis and influencing the capacity to block protons. The internal pH change interferes also with DNA transcription [5, 6].

The antibacterial activity of *Mentha* species in particular, is mainly attributable to the presence of phenols and terpenoids [7]. Menthol and menthone, compounds contained in high percentage in *Mentha piperita* (peppermint) oils, show, as well as other monoterpenes, a strong antibacterial activity. Combination of menthol with antibiotics, such as oxacillin,

promotes synergistic antibacterial effects probably due to the increase of membrane permeability related to menthol action [8].

Despite of the increasing interest in EO properties, very few studies on functionalization of solid surfaces with these molecules are reported in literature [9 – 21].

The novelty of the present work is coupling molecules from peppermint EO to the surface of a chemically-treated titanium alloy, suitable for biomedical (such as bone contact implants) or different applications (general purposes objects, laboratory instruments) to reduce bacterial adhesion.

The specific peppermint EO used in this study was selected after that other EOs (i.e. Thymus Vulgaris, Lavandula Hybrid) have been tested against a biofilm-forming Sthaphylococcus aureus strain: Peppermint EO was found to possess the most pronounced staphylococcal inhibitory activity.

Moreover, since there are no consolidated protocol in literature for the characterization of surfaces modified with EOs, a procedure for a proper characterization of these materials is here suggested.

2. Materials and methods

2.1 Surface chemical treatment

The substrate selected for the surface modification was titanium alloy Ti6Al4V (ASTM B348, Gr5, Titanium Consulting and Trading, discs 10 mm in diameter). All the discs were polished with SiC papers (up to 4000 grit). Polished discs were used as reference materials.

In order to make bioactive the surface, to expose OH groups and to increase roughness on a nanometric scale, as needed for functionalization and coating, the samples were subjected to a patented chemical treatment [22, 23] that consists in acid etching in diluted hydrofluoric acid and controlled re-oxidation in hydrogen peroxide.

The treated samples were UV irradiated to reduce carbon contamination before functionalization and to improve the reactivity of OH groups. These samples will be named chemically-treated (CT) from now on.

2.2 Grafting of natural molecules: functionalization or coating

Following two different protocols, the surface was coated or functionalized with peppermint (*Mentha piperita)* Essential oil (Mentha EO, EssenzialMenta, Pancalieri, Italy)~~, which was selected in view of its antibacterial properties as well as of its peculiar local production which can support regional development~~.

A drop of the EO was spread on the surface of the sample CT and then polymerized at 37 °C for 48 h to obtain a coating. After that time, the samples were washed in ultrapure water and then left drying at room temperature. These samples were named CT_Mentha oil.

Functionalization (that means grafting of molecules to the surface without formation of a continuous coating) was performed by using a solution with concentration 50% v/v Mentha EO in ethanol. The samples were soaked in this solution for 48 h at 37°C and then washed in ethanol, in ultrapure water, dried at room temperature and preserved in the dark. The obtained samples were named CT_50%Mentha oil (soaking).

2.3 Fluorescence microscope observation

Presence and distribution on the CT sample surface of compounds from the peppermint EO were investigated by fluorescence microscopy based on triplicate measurements (Leica DM5500 BLeica Microsystems, Basel, Switzerland) exploiting the autofluorescence of EOs [24].

2.3 Gaschromatographic-Mass Spectrometry (GC-MS) analysis

Gaschromatographic analyses were performed on pure EOs (based on triplicate measurements) and on solutions containing the detached compounds from the coated/functionalized samples (as described in the following) to understand which molecules from the EO could bind to the surface of the CT sample.

After coating/functionalization, the compounds deriving from EO grafted to the sample surfaces were detached by sonicating each sample in 3 ml of absolute ethanol for 10 minutes. Following the addition of 3 ml of MilliQ water and 1 ml of *n*-hexane, the solutions from sonicated samples were mixed vigorously by vortexing for 20 sec and then centrifuged at 1000 RPM for 5 min using a table top centrifuge. The organic upper phase was then dehydrated in a glass column packed with anhydrous magnesium sulphate (Fluka, USA) and concentrated by a constant flow of nitrogen (N_2) to 100 µl before GC-MS analysis. In total 3 µl of each concentrated sample were injected in the gaschromatograph and the identification of compounds was based on the comparison of their mass spectra with NIST 98 by the NIST v2.0 research software.

Qualitative and quantitative analyses of the different compounds were carried out on an Agilent 6890N gas chromatograph coupled to Agilent 5973A mass spectrometer. The GC was equipped with a HP5-MS column (30 m length, 250 µm diameter, 0.25 µm thickness). Helium was used as carrier gas at constant flow of 1 ml min^{-1}. The following temperature program was used: 60°C as initial temperature, thermal gradient of 3°C min^{-1} up to 250°C. Post time lasted 2 minutes at 250 °C. Injector port was set at 250°C in splitless mode. Transfer line temperature to MSD was 280 °C and ionization energy (EI) was 70 eV. Mass spectra were acquired in full scan mode with 50 – 350 m/z range.

2.4 Contact angle

The surface wettability was evaluated by means of triplicate measurements of the contact angle with sessile drop method before and after functionalization/coating. Each sample was

placed on the support of the microscope (Kruss DSA 100) in front of the camera with the treated side upward and a drop of 5 µl of ultrapure water was deposited with a micropipette on the surface. The images were acquired with the camera and elaborated by the software obtaining the value of the contact angle. The measures were performed in triplicate on each kind of samples produced. Mean and standard deviation were calculated for each set of samples and data have been analyzed by means of one-way ANOVA, with a significance level $p<0.05$.

2.5 Fourier Transformed Infrared spectroscopy (*FTIR) analysis*

Fourier Transformed Infrared spectroscopy (FTIR, FTIR Hyperion 2000 - Tensor 27, Bruker Optics, Ettlingen, Germany) analysis in reflectance mode was performed to check the chemical groups on sample surface before and after functionalization/coating and to verify the presence of compounds from the EO. Spectra were acquired in duplicate between 400 and 4000 cm^{-1}. The spectrum of the pure EO was instead acquired in ATR mode (Attenuated Total Reflectance - FTIR Alpha, Bruker Optics, Ettlingen, Germany) between 400 and 4000 cm^{-1}.

2.6 *X-ray Photoelectron Spectroscopy (XPS) analysis*

X-ray Photoelectron Spectroscopy analysis (XPS, PHI 5000 VERSAPROBE, PHYSICAL ELECTRONICS) was performed in duplicate to determine the chemical groups on the surface before and after the coating/functionalization and to confirm the presence of molecules of the essential oil.

2.7 Z potential electrokinetic measurements

The surface charge in function of pH before and after functionalization/coating was analyzed by means of electrokinetic measurements (SurPASS, Anton Paar).

A couple of samples was prepared for each type and the surface z potential was determined in function of pH in a 0.001 M KCl electrolyte solution (titration curve). The pH value was varied by adding 0.05 M HCl or 0.05 M NaOH using the instrument titration unit [25].

2.8 Tape test

Tape test, performed in accordance with the standard ASTM D 3359 [26], was used to evaluates the adhesion of coating films to metallic substrates; it was performed in duplicate by applying and removing a strip of pressure sensitive tape over the coating. Standard cutting were made on the coating film with a sharp razor blade before the test.

The tape test was performed on the CT_Mentha oil samples. The degree of coating adhesion was evaluated by means of macroscopic and optical microscopy observations.

2.9 In vitro microbiological tests

Two different tests were performed with bacteria in order to (i) investigate the ability of mint oil to limit bacterial adhesion and (ii) its ability to reduce biofilm formation.

All the specimens for microbiological tests were sterilized by means of UV-C irradiation. In the case of coated/functionalized samples, then the surface grafting was performed in sterilize containers and clean environment (Faster Cytosafe- N 2003).

2.9.1 Bacterial strain

A commercial *Staphylococcus aureus* strain was acquired from the American Type Culture Collection (ATCC, Manassas, VA, USA, reference strain 29213) and used for all the microbiological assays as periprosthetic infection representative microbiological agents. The strain was cultured on Mannitol salt agar (Merck, Darmstadt, Germany), and young colonies (18–24 hours) were inoculated into cryovials and maintained at -80°C for extended storage [27]

2.9.2 Peppermint essential oil minimum inhibitory concentration (MIC) determination

The direct effect of the peppermint EO on staphylococcal growth was tested according to European guidelines (http://www.eucast.org/ast_of_bacteria/mic_determination/?no_cache=1) ~~EUCAST Guidelines, www.eucast.org).~~ The MIC by using 2-fold dilutions of peppermint EO from 2% v/v in Mueller Hinton broth (Becton Dickinson and Company, BD, New Jersey, USA) and tween 80 (0.001% v/v), has been performed in microtiter plates and assigned as the lowest concentration that inhibits visible staphylococcal growth after overnight incubation at 37°C.

2.9.3 Inhibition halo assay

To test the release of peppermint EO from treated sample discs and its effect on staphylococcal growth, an agar inhibition halo assay was performed inoculating staphylococci, at about 10^8 colony forming unit (CFU)/ml, on Mueller Hinton agar (Sigma-Aldrich, Missouri, USA) before sterile disc placement. Then, the plates were incubated for 24h at 37°C and the inhibition zone diameter around the disc was measured (mm) to compare the antimicrobial efficacy of treated and untreated samples.

2.9.4 Staphylococcal adhesion tests

Bacterial adhesion test was performed to evaluate the quantity of adherent bacteria on different disc samples after 24h of incubation in the presence of staphylococci. Nine samples for each type were prepared and tested. Briefly, each sample was immersed in a 10^4 CFU/ml bacterial suspension in Mueller Hinton broth (BD), and incubated at 37 °C overnight; after then, the discs were removed, posed into sterile plastic bags containing NaCl 0.9 w/v % (Bieffe Medital S.p.A., Grosotto, Italy) and subjected to a 7 min sonication (40 kHz) to detach adhered bacteria. Both the adhered and planktonic cells, referred to each sample, were plated

on Nutrient agar (Biolife Italiana, Milan, Italy) and counted as CFU/ml [~~1,~~ 28, 29]. The adhesion experiments were performed in triplicate and repeated a minimum of three times.

2.9.5 Biofilm formation assays

Sterile specimens (in triplicate) were placed in a 24 multiwell plate (Nunclon Delta Surface, Thermo Scientific) and submerged in 1 ml of Luria Bertani medium (LB, from Sigma, Milan, Italy) containing $1x10^5$ UFC/ ml corresponding to 0.01 optical density at 600 nm wavelenght. The plate was incubated for 90 minutes at 37°C under agitation at 120 rpm (adhesion phase). Supernatants were then extracted to remove floating planktonic cells (separation phase) and specimens gently washed 3 times with PBS (Phosphate Buffer Saline, Sigma-Aldrich, P4417) to remove non-adherent cells [30, 31]. Then, each specimen was rinsed with 1 ml of fresh LB medium and plate incubated for 24, 48 and 72 h at 37°C for biofilm cultivation.

To assess the bacterial growth capacity after 24, 48 and 72 h of direct contact compared to that of untreated controls, bacterial viability was evaluated by the validated quantitative colorimetric metabolic 2,3-bis (2-methoxy-4-nitro-5-sulphophenyl)-5-[(phenyl amino) carbonyl]-2H-tetrazolium hydroxide assay (XTT, Sigma-Aldrich). Briefly, 20 µL of XTT solution (3 mg mL−1 in acetone containing 0.1M menadione) were added to each well and plates were incubated at 37°C for 5 h in the dark. Then, 50 µL were collected from each well and centrifuged for 2 min at 480 g to remove any debris, and the optical density was evaluated using a spectrophotometer (Spark, Tecan, Männedorf, Switzerland) at 490 nm. ~~Mirror-~~ Polished specimens were considered as control.

To determine the bacteria viability a Live/Dead BacLight bacterial viability kit (Molecular Probes, Life Technologies Italia, Monza, Italy) was used. The kit includes two fluorescent nucleic acid stains: SYTO9 and propidium iodide. SYTO9 penetrates and stains both viable and nonviable bacteria, while propidium iodide enters only damaged/dead cells and quenches SYTO9 fluorescence.

For assessing viability, 1 mL of stock solution of each stain was added to 3 mL of PBS and, after mixing, the solution was distributed into the plates containing the material specimens and incubated at room temperature for 15 min in the dark. Stained biofilms were examined by fluorescent microscope (Leica 6500, Leica Microsystems, Basel, Switzerland). Finally, the number of dead bacteria was calculated and expressed as % of total bacteria number by ImageJ (NIH, Bethesda, USA) software.

2.9.6 Statistical analysis

The adhesion assay results (mean ± SEM) were tested by the unpaired t-tests (Graphpad Software, San Diego, CA, USA). While anti-biofilm formation results were analysed by ONE-way ANOVA followed by the Tukey's post-hoc analysis. A $p< 0.05$; 95% confidence interval was judged to be significant.

3. Results

3.1 Macroscopic observations

The Ti6Al4V samples turn from metallic grey to changing purple-green after the surface chemical treatment (CT samples) because of formation of a surface layer of titanium oxide thicker than the native one (200-300 nm), as reported in [23, 32].

After the procedure of coating, a layer of a transparent coating is visible on the surface for the sample CT_Mentha oil.

For the functionalized samples CT_50%Mentha oil (soaking), no change is visible at macroscopic level by comparing the samples before and after functionalization, as reported in Figure 1.

3.2 Fluorescence microscope observation

The images obtained with the fluorescent microscope are reported in Figure 2.

The image of the CT sample is dark because, as expected, it is not fluorescent, while the samples treated with the peppermint oil appear red colored (with different intensities and distribution of color) due to the presence of fluorescent molecules [24]. The CT_Mentha oil sample has an almost uniform fluorescence due to the presence of a continuous layer of polymerized oil. The functionalized samples CT_50%Mentha oil (soaking) show a less intense fluorescent halo on the whole surface with fluorescent spots highlighting the grafting of biomolecules from the oil to the CT substrate without formation of a thick continuous coating.

3.3 GC-MS analysis

GC-MS analyses were performed on pure EO and on solutions containing the biomolecules detached from the samples after coating/functionalization to identify the compounds deriving from the oil.

The analysis performed on the pure EO is reported in Table 1.

The main compounds of the peppermint EO are 1,8-Cineol (Eucalyptol), menthone, menthofuran, -(-)-menthol, camphane and trans-caryophyllene. The oxygenated compounds are the 88.7%, while terpene hydrocarbons are 11.47%. Menthol, menthone and trans-caryophyllene are of interest because of their antibacterial and anti-inflammatory effects [33].

The results obtained through gaschromatographic analysis on the biomolecules detached from the coated/functionalized samples are reported in Table 2. The coated samples contain menthol, hydroxyl-menthofuran, menthyl-acetate and β-cubebene, while the functionalized ones contain β-cubebene and trans-caryophyllene.

Menthol, menthyl-acetate and trans-caryophyllene are among the components of the peppermint EO used for grafting, as reported in Table 1. Hydroxyl-menthofuran is a metabolite of menthofuran, which is a component of the peppermint EO, and β-cubebene is an

isomer of α-copaene, also a component of the peppermint EO [34]. The presence of this compound could be correlated with a rotation of the molecule during functionalization and grafting to the surface or during extraction from the surface.

3.4 Contact angle measurements

The mean values of contact angle measured on the sample surfaces and their standard deviations are reported in Table 3.

The chemical treatment significantly decreases ($p<0.05$) the contact angle of the titanium alloy both because of OH groups exposed on the surface after the treatment and nanotopography of the oxide layer [23]. Water wettability of the CT samples after coating/functionalization decreases because of the presence in the oil of organic compounds with hydrophobic domains. Both for coating and functionalization the increase in the contact angle value is statistically significant ($p<0.05$). The presence of apolar compounds on the surface of the functionalized samples, as detected by gaschromatographic analysis, is in agreement with the measured high hydrophobicity of this surface.

3.5 FTIR

FTIR analyses were performed on the pure liquid EO and on CT samples before and after coating/functionalization. The obtained spectra are reported in Figure 3.

Figure 3A displays the complex vibrational pattern of the peppermint oil, arising from the vibrational modes of the several components of the oil mixture. The abundance of oxygenated monoterpenes is confirmed by the observed modes, mainly related to aliphatic/alicyclic and aromatic compounds rich in hydroxyl and carbonyl functional groups, in agreement with the results of the gaschromatographic analysis. The main peaks with corresponding attributions are listed in Table 4.

The spectrum of the pure liquid oil shows several peaks which are useful as comparison for identifying the molecular species grafted to the functionalized surfaces or making the coating (Figure 3B). As a first glance, the spectra recorded on the surfaces treated with the peppermint oil confirm that the coating/ functionalization treatments have been successfully carried out.

The band between 3450-3200 cm^{-1} of the OH stretching [39] is detected on all the samples and it is mainly related to the OH groups of the surface oxide layer of the chemically treated substrate, even if a contribution can be derived from the alcoholic compounds of the peppermint oil, such as -(-)-Menthol, on the coated samples.

The spectrum of the CT_Mentha oil sample is significantly different from the spectrum of the CT sample, evidencing the presence of the coating, but it is difficult to identify with certainty each peak because the thick and semitransparent coating originates internal reflections of the IR light, creating interferential effects on the signal.

Nevertheless, it was possible to observe on the coated sample peaks between 2960-2870 cm^{-1} due to the stretching vibration of C-H aliphatic bonds [36] (Figure 3-b1) and a peak between 1780-1700 cm^{-1} due to C=O stretching [35] (Figure 3-b2). These peaks were absent on the spectrum of the CT sample and are correlated with the presence on the substrate of the grafted biomolecules from the oil.

For the functionalized samples, the peaks between 2960-2870 cm^{-1} are less evident because, in this case, there is not a continuous coating, but only ~~a thin layer of~~ biomolecules grafted to the substrate.

For all the coated/ functionalized samples, the peak around 1450 cm^{-1} could be correlated with the bending of aliphatic C-H, but also to the in plane deformation of CH_2 groups with a C atom involved in a C=C bond [41], such as in the molecules detected by gaschromatographic analysis (trans-caryophyllene).

3.5 XPS

XPS analyses were performed on the samples before and after coating/functionalization in order to investigate the elements on the surfaces and the chemical groups exposed. The atomic element percentage, as detected in the survey spectra, are reported in Table 5.

Regarding the coated samples (CT_Mentha oil), it is evident that the titanium alloy substrate is not detectable because of the thick coating on the surface. The percentage of carbon grows considerably, with respect to the CT sample, because of the presence of the organic layer, whereas the percentage of oxygen decreases because of the titanium oxide hydroxylate layer is no more detectable. For the functionalized samples CT_50% Mentha oil (soaking), the chemically treated titanium alloy substrate is still detectable because of the absence of a continuous and thick coating. Furthermore, on these samples an increase of the carbon percentage and a decrease of the oxygen percentage are visible, in a lower quantity if compared with the coated samples, which can be correlated with the presence of single molecules grafted to the substrate. For a better understanding of the chemical groups on the sample surfaces, high resolution analysis of the carbon and oxygen regions was performed.

In the carbon region (data not shown), the same four peaks are detected for all the samples. A peak at 284 eV correlated with C=C bonds [42] is present for all the samples, but it is higher for the samples CT_50%Mentha oil (soaking) due to the presence of beta-cubebene and trans-caryophyllene on the surface. A peak around 285.2 eV is detected due to C-C and C-H bonds [43–45] and it can be mainly ascribed to unavoidable atmospheric contamination, always present on titanium surfaces in the case of CT or to the presence of organic molecules grafted from the oil in the other cases.

Two peaks at 286 eV and 288.5 eV are detected due r to C-O and C=O bonds[45] respectively that could be again correlated both to contaminants or to the molecules grafted from the oil. Because of the presence of similar carbon bonds in the atmospheric contaminants and in the compounds of peppermint oil, the analysis of the carbon region alone is not enough to

highlight significant differences between the samples. The oxygen region is much more significant and the spectra are reported in Figure 4.

The spectrum of the CT sample (Fig. 4a) shows the characteristic peak of titanium oxide at 530 eV, and the peak associated to OH groups (Ti-OH) at about 532 eV [22, 46]. Different peaks are observable in the high resolution spectra of the specimens CT_Mentha oil (Fig. 4b): a first one, that appears at 532 eV, can be associated to aliphatic C=O bonds (the attribution to OH groups of the Ti substrates is excluded because titanium is not detected in the survey spectrum), while the second one at 533 eV is related to C-O bonds [44, 47]: both peaks can be associated to the presence of the polymerized compounds deriving from EO. These results highlight the presence of the compounds of the peppermint oil in the coating. Regarding the functionalized samples CT_50% Mentha oil (soaking) (Fig. 4c), two peaks at 530 eV and 532 eV are present: the first is correlated with the Ti-O and the second with Ti-OH bonds [46, 48], characteristic of the CT substrate. The peak at 532 eV could be also due to C=O bonds of the grafted biomolecules [44, 47] but in this case, on the basis of gaschromatographic analysis, which did not show the presence of compounds with C=O groups, can be excluded.

3.6 Z potential electrokinetic measurements

The titration curves of the CT and coated/functionalized samples are reported in Figure 5. The principal results obtained from the curves are summarized in Table 6.

The coated/functionalized samples show a shift of the isoelectric point (IEP) compared with the CT samples confirming the success of both the grafting procedures: the position of the IEP depends on the balance on the surface of acidic and basic functional groups and it is changed by the presence of the grafted biomolecules.

The samples CT_Mentha oil have a negative z potential for pH>3 with a constant decreasing trend and high slope of the titration curve: this behavior is typical of hydrophobic surfaces. As much as the solution in contact with the surface becomes more reach in OH groups (by

increasing pH), more OH groups are adsorbed on the surface instead of water molecules (which are weakly adsorbed because of hydrophobicity) and the surface has a negative surface charge increasing in absolute value because of the increasing amount of adsorbed hydroxyl groups instead of water molecules.

The value of the IEP of the coated surface suggests that some acidic functional groups are in the coating (IEP is expected to be around 4 for a surface without any functional groups or with a balance between acidic and basic ones). The absence of a plateau in the range pH 6-8 suggests that these groups act as a very weak acid and they are completely dissociated only at very high pH (the onset of a plateau is observable at pH>9): when a surface shows functional groups completely dissociated, no more hydroxyl groups are adsorbed from the solution even if pH increases because of the stronger bond with the adsorbed water molecules and repulsion between negative charges.

On the other side, the wide plateau detected on the samples CT in the range pH 6-8, the very low IEP and the lower slope of the curve around IEP suggest the presence on the surface of chemical groups of the same type (OH groups) with a strong acidic behavior [49] exposed by the substrate as a consequence of the chemical treatment [22, 23]. The great difference between the curves of CT and CT_Mentha oil evidences that the coating completely covers the surface and the CT substrate is no more exposed to the solution during the titration test.

The functionalized sample CT_50% Mentha oil (soaking) is alike the coated sample CT_Mentha oil in the acidic range, confirming the presence of the grafted biomolecules from the oil; there is a similarity with the CT samples in the basic range because of the absence of a thick and continuous coating, even if the presence of the grafted molecules affects the slope of the curve in the range pH 6-8 with respect to the CT sample.

3.7 Tape test

The samples CT_Mentha oil were tested with the tape test to evaluate the coating adhesion to the substrate. The aspect of the coating before and after the test at optical microscope observations is reported in Figure 6.

Figure 6 shows that the peppermint oil coating has good adhesion to the underlying material: although the oil partially adheres to the tape, it remains also attached on the sample in the test area. In addition, the detachment of the oil coating from the underlying material occurs in the form of bubbles. This form of separation is known as boiling. The adhesion can be classified as 4B/5B in accordance to standard ASTM D 3359: the damage indeed is limited to the incision area [26].

3.8 In vitro microbiological tests

The adhesion test results performed by using *S. aureus* ATCC 29213 (MIC=0.25% v/v peppermint EO) on the samples treated with peppermint oil and expressed as CFU/ml are reported in Figure 7. The CT and ~~smooth~~ polished Ti6Al4V samples were used as control series.

The adherent bacteria medium amount on the control samples after 24h of incubation is $1.44*10^8$ CFU/ml and $1.19*10^8$ CFU/ml for Ti6Al4V and CT, respectively. For the samples treated with the peppermint oil, the count results about an order of magnitude minor and it is respectively $2.46*10^7$ CFU/ml for the CT_Mentha oil samples and $5.00*10^7$ CFU/ml for the CT_50%Mentha oil (soaking) samples. The reduction of the adherent bacteria for the coated and functionalized samples is significant ($p<0.01$ and $p<0.05$) and it is greater for the samples CT_Mentha oil because of the higher amount of antibacterial chemical compounds as highlighted by gaschromatographic analysis (phenols and terpenoids).

No antibacterial effect was noted on the planktonic bacteria, resulting in an order of magnitude of 10^9 CFU/ml for all the samples, revealing that, as expected, no release of

antibacterial agents occurs in aqueous media by the coated/functionalized surfaces, as also demonstrated by the absence of an inhibition halo (data not shown).

According to the obtained results, specific tests for biofilm growth ability on the CT_Mentha oil and CT_50%Mentha oil (soaking) samples were performed and the obtained results are reported in Figures 8 and 9 (CT and ~~smooth~~ polished Ti6Al4V samples were used as controls).

The use of the oil was successfully in reducing bacteria viability only when it is applied as a coating (Figure 8a-b-c); in fact, significant results were achieved on the CT_Mentha oil samples after 24-48-72 hours in comparison with CT ($p<0.05$, indicated by the *) and after 24 and 72 hours in comparison with CT_50%Mentha oil (soaking) samples ($p<0.05$, indicated by the §). Conversely, when functionalization procedure was used (samples named CT), the killing effect was noticeably reduced after 24 hours while it was increased in the following 48 and 72 hours.

Finally, the results were expressed as optical density in function of time (Figure 8d) and as percentage of bacteria viability in comparison with ~~smooth~~ polished Ti6Al4V (Figure 8e). Accordingly, it was possible to notice that bacteria viability was increased during the 72 hours experimentation, thus suggesting a bacteriostatic effect due to the oil coating rather than a bactericidal effect; moreover, biofilm cells viability was never lowered until < 40-50%.

Data obtained by XTT analysis were confirmed by the Live/Dead assay (Figure 9). ~~In fact, the number of dead bacteria (stained in yellow/red) markedly increased on the coated samples, while a minor effect was observed on the functionalized ones where bacteria resulted as mainly viable (stained in green).~~

In fact, onto the surface of control CT samples, a homogeneous layer of viable bacteria (stained in green) was found to be adhered as single colonies as well as biofilm clusters. When the 50% oil was applied (CT_50%Mentha oil), a marked decrease of viable bacteria density was noticed in comparison with the CT ones as well as numerous dead colonies

(stained in red) were detected; finally, the treatment with undiluted oil (CT_Mentha oil) determined a further decrease of viable adhered bacteria in comparison with the CT_50%Mentha oil and the higher number of dead colonies between all the tested specimens was here detected.

4. Discussion

The context of this work is the medical and industrial need of antimicrobial surfaces treated with alternative agents with respect to antibiotics. EOs have a great potential on this concern, but their scientific and systematic testing has not been completely covered till now, as well as their use not as liquid or food supplement, but in coupling to a surface. For examples, *Salvia officinalis* EO was coupled as nanoparticles on the surfaces of a prosthetic implant to avoid biofilm formation [9]; cinnamon EO was used to coat stainless steel orthopedic prosthesis [10] and, encapsulated in a sol-gel, it produces hybrid silica matrix with antibacterial effects [14]; *Artemisia mesatlantica* EO and *Mentha spicata* EO were adsorbed on steel to avoid corrosion [15, 50]; oregano EO was used to functionalized alginate film to increase elongation at break and thickness conferring at the same time antibacterial properties [17]; carvacrol and thymol isolated from the *Origanum dictamnus* and *Artemisia arborescens L.* EOs were liposomal embedded to preserve their antiviral ad antibacterial activities [18, 19]; menthol-PCl micro and nanoparticles were used for cotton tissue functionalization to avoid bacterial and fungal contamination [20]; magnetic nanoparticles were coated with *Eugenia caryophyllata*, *Anethum graveolens*, *Salvia officinalis* and *Mentha piperita* EOs [21, 11, 51]; thyme oil was encapsulated in chitosan and benzoic acid-based nanogel to preserve its antifungal activity [12] and *Mentha spicata L.* EO was encapsulated in chitosan matrix to relieve skin irritation [13].

In this research, a chemically treated titanium alloy substrate (CT) has been selected for coating and functionalization. The CT surface has an oxide layer with topography on the

nanoscale, sponge appearance (pores below 10 nm) and high density of OH groups, as described in [22]. This type of surface treatment was selected because the occurrence of both nano-pores and OH functional groups can enhance the grafting ability of the surface with respect to biomolecules and coatings, as described in [52].

Observations through fluorescent microscopy evidence the presence of a continuous thick coating on CT_Mentha oil and the presence of ~~a molecular layer~~ grafted molecules on CT_50%Mentha oil (soaking). The compounds grafted in both cases were analyzed through gaschromatophy. The coating on the CT_Mentha oil samples is composed by menthol, hydroxyl-menthofuran, beta-cubebene and menthyl-acetate. It has a prevalence of oxygenated species, differently to the peppermint oil, probably because the compounds with higher ability to polymerize are selected by the process. For instance, menthone is absent from the coating even if it is one of the main component of the peppermint oil because, if not chemically modified, it does not polymerize, [53]. Moreover, a temperature of 37°C was selected for grafting because it was previously showed that it enhances the grafting ability of the CT surface [52] and it is closed to physiological temperature. In the specific case of coating/functionalization by using EOs, temperature induces a further selection of the compounds bind to the surface with loss of the most volatile ones (such as cineol, camphane): in fact, all the compounds of the coating/functionalized surfaces belong to the fraction of the compounds deriving from the oil with higher boiling temperature (higher than 200°C).

The grafted compounds by functionalization procedure [CT_50%Mentha oil (soaking) samples] are apolar and not oxygenated (β-cubebene and trans-caryophyllene) and it is interesting to note that these compounds are minority fractions of the peppermint oil. The selected combination of the functionalization procedure and chemical affinity for the treated titanium surface acts as highly selective with respect to the complex mixture of compounds of the peppermint oil: high affinity between titanium and carbon, coupled with low affinity of the apolar biomolecules with the used solvents (water and ethanol), high boiling

temperature/low vapor pressure (as low as 0.013 mmHg at 25°C) are the concurrent factors affecting selective grafting. On the other side, chemical interaction between the oxygenated functional groups of the organic compounds of the oil and the hydroxyl groups on the surface seems to be ineffective for functionalization. In conclusion, the antibacterial compounds, such as phenols and terpenoids, are much more easily grafted through coating than by grafting.

Contact angle, FTIR, XPS and zeta potential analyses are useful for confirming these results by direct analysis of the coated/functionalized surfaces: a good agreement was found in this research about the collected data.

Zeta potential titration curves require a much more detailed discussion. As first, the presence of grafted biomolecules on the coated and functionalized surfaces is confirmed by the shift of IEP with respect to the CT sample. As second, IEP of the coated surface is in agreement with the GC-MS data and the presence of compounds with weak acidic functional groups, such as menthol and hydroxyl-menthofuran. As last, the hydrophobic behavior of the coated surface is in agreement with the presence of a continuous coating of organic compounds with hydrophobic domains, while the functionalized sample CT_50% Mentha oil (soaking) has not a continuous coating and the zeta potential curve obtained is due to the exposition to the test solution of both the substrate (CT) and grafted biomolecules, confirming fluorescence images.

~~The coated/functionalized samples show a shift of the isoelectric point (IEP) compared with the CT samples confirming the success of both the grafting procedures: the position of the IEP depends on the balance on the surface of acidic and basic functional groups and it is changed by the presence of the grafted biomolecules.~~

~~The samples CT_Mentha oil have a negative z potential for pH>3 with a constant decreasing trend and high slope of the titration curve: this behavior is typical of hydrophobic surfaces. As much as the solution in contact with the surface becomes more reach in OH groups (by increasing pH), more OH groups are adsorbed on the surface instead of water molecules~~

~~(which are weakly adsorbed because of hydrophobicity) and the surface has a negative surface charge increasing in absolute value because of the increasing amount of adsorbed hydroxyl groups instead of water molecules. The value of the IEP of the coated surface suggests that some acidic functional groups are in the coating (IEP is expected to be around 4 for a surface without any functional groups or with a balance between acidic and basic ones): this is in agreement with the presence of menthol and hydroxyl menthofuran within the coating (OH groups). The absence of a plateau in the range pH 6-8 suggests that these groups act as a very weak acid and they are completely dissociated only at very high pH (the onset of a plateau is observable at pH>9): when a surface shows functional groups completely dissociated, no more hydroxyl groups are adsorbed from the solution even if pH increases because of the stronger bond with the adsorbed water molecules and repulsion between negative charges.~~

~~On the other side, the wide plateau detected on the samples CT in the range pH 6-8, the very low IEP and the lower slope of the curve around IEP suggest the presence on the surface of chemical groups of the same type (OH groups) with a strong acidic behavior [53] exposed by the substrate as a consequence of the chemical treatment [22, 23]. The great difference between the curves of CT and CT_Mentha oil evidences that the coating completely covers the surface and the CT substrate is no more exposed to the solution during the titration test.~~

~~The functionalized sample CT_50% Mentha oil (soaking) is alike the coated sample CT_Mentha oil in the acidic range, confirming the presence of the grafted biomolecules from the oil; there is a similarity with the CT samples in the basic range because of the absence of a thick and continuous coating, even if the presence of the grafted molecules affects the slope of the curve in the range pH 6-8 with respect to the CT sample.~~

Tape test was used for a preliminary investigation of the adhesion of the coating with promising results.

A significant reduction of the adherent staphylococci and biofilm formation was found mainly on coated samples because of the higher amount of grafted antibacterial compounds (phenols

and terpenoids) in agreement with gas-chromatographic analysis. These compounds are known to be wide-range antibacterial agents due to their activity targeted towards different mechanisms. The ability to counteract the biofilm formation is related to the phenols ability to interfere with the N-acylhomoserine lactone-mediated quorum sensing signaling that is fundamental for the recruitment of floating bacteria [54, 55]. Moreover, the presence of surface-grafted phenols can decrease the ability of bacteria to successfully adhere by mimicking the lipopolysaccharide (LPS) binding site [54]. As a consequence, the LPS binding to the grafted phenols might lead to the destabilization of the outer membrane of the bacteria, thus making their membranes more permeable to antibacterial compounds as well as their inner systems more defenseless.

A significant reduction of the adherent staphylococci and biofilm formation was found mainly on coated samples because of the higher amount of grafted antibacterial compounds in agreement with gaschromatographic analysis. These results could be applied to all types of peppermint oil, previous MIC determination on bacterial strains. This preliminary characterization evidences the antibacterial capacity ~~potential~~ of this type of surface grafting; it could be of interest for application in different biomedical fields (such as bone contact) or general purpose objects and laboratory instruments. Cytocompatibility with respect to different cell phenotypes has to be evaluated case by case according to the specific application selected. ~~even if a much more detailed work is needed~~ ~~to identify for which type of industrial or biomedical application it can be suitable~~. In the case of the functionalization process the possibility of coupling this strategy to other antimicrobial agents should be considered.

In medical field, biomaterials associated infection (BAI) is the most common issue associated with implants regardless of their form or function. Bacteria form colonies and this result in the formation of biofilm on the surface, making the infection unreceptive to antibiotics and host defense mechanisms, with implant removal as outcome [27-29]. Medicinal plants have widespread usage for their active biomolecules, and the study of their antimicrobial activities,

similar to those of traditional antibiotics, but with the vantage of a low capability to induce bacterial resistance, has gained widespread importance. The exact antibacterial mechanisms have to be deeply understood and they may be could be attributed to several targets in the bacterial cell. Thus, the strategy of EO coating on biomaterial surfaces could significantly reduce BAI.

In this research, for the first time, a protocol for characterization of EO grafted on solid substrates was developed. It has proved to be robust and appropriated; the suggested tests are necessary and complementary, providing solidly proved results. The use in combination of the suggested techniques allows to understand which compounds are present on the surfaces (by matching GC-MS, FTIR, XPS, contact angle and zeta potential data), how they are distributed (by matching fluorescence microscopy images and zeta potential data) and to characterize their mechanical (by tape test) and chemical stability in contact with solutions (by zeta potential data). Then, the selected microbiological tests allow to investigate not only the ability to limit bacterial adhesion, but also to reduce biofilm formation. In fact, the CFU count was useful to confirm that the coating was able to reduce the number of adhered bacteria thus demonstrating the anti-adhesive ability prior mentioned. Then, the metabolic evaluation exploited by XTT assay demonstrated that the metabolism of adhered bacteria was significantly lowered by the presence of mentha oil active compounds; finally, Live/Dead staining gave a visual confirmation of the previous data as the coated surfaces displayed a lower number of viable bacteria than the CT controls and a higher percentage of dead colonies thus demonstrating a reduction in terms of both number and metabolically active bacteria.

All these data provide a comprehensive scenario useful for a first evaluation of the potential of the investigated surfaces against bacterial colonization issues.

5. Conclusions

Surface modification of Ti6Al4V alloy with peppermint EO was performed for the first time in this research. An oil coating was created on the surface of chemically treated Ti6Al4V samples by polymerization of peppermint oil and surface functionalization was performed by means of soaking in an ethanol solution of the oil. In the first case, a homogeneous and continuous coating is obtained containing a prevalence of oxygenated compounds (menthol, hydroxyl-menthofuran and menthyl-acetate). The coating was investigated by means of tape tests and shows strong adhesion to the substrate.

On the surface of the functionalized samples, the presence of two non-oxygenated grafted compounds (trans-caryophyllene and beta-cubebene) was detected without the formation of a coating. The surface of the CT samples combined to the selected functionalization procedure are selective towards some specific not oxygenated compounds even if they are minority fractions in the source peppermint oil.

~~The antibacterial tests performed highlighted that the coating has an effect on both the bacterial adhesion and subsequent biofilm formation, that is lower on the functionalized samples.~~ The obtained results highlighted bacteriostatic effects of peppermint EO on Gram-positive bacteria. Thus, peppermint EO could be considered a promising coating on the implant surfaces to prevent bacterial adhesion and biofilm formation that is lower on the functionalized samples.

~~Despite a wide research on pure EOs, the works on surface grafting of these molecules are still few in the scientific literature with consequent lack of knowledge on their characterization. In this research, for the first time, a protocol for the characterization of EO grafted on solid substrates was developed. The use in combination of fluorescence microscopy observation, FTIR, XPS, zeta potential and GC-MS analyses, as well as contact angle and tape tests, seems to be a good protocol to characterize this material type: it allows to understand which compounds are present on the surfaces, how they are distributed on the~~

~~surface after the coating or functionalization procedures and to characterize their mechanical and chemical stability/reactivity.~~

After these first attempts, combining the properties of EOs with those of the metallic materials seems to be a promising way to reduce bacterial adhesion on prosthetic implants, biomedical devices or surfaces for everyday use even if a wide scientific work is needed to select the much more promising oils, the procedures to be used and cytocompatibility of the treated surfaces.

Acknowledgements

This work was in part supported by a research grant from Fondazione Cassa di Risparmio di Torino (RF=2015.1681).

Authors' contribution:

C. M. Bertea, S.Ferraris, A. Cochis, M. Cazzola, V. Allizond: experimental design, carrying out measurements, manuscript composition

C. Novara: carrying out measurements, manuscript composition

F. Geobaldo, L. Rimondini: experimental design, manuscript composition

A.M. Cuffini, A. Bistolfi: medical input and conception

G. Banche, S. Spriano: conception, experimental design, manuscript composition

References

[1] Chouirfa H, Bouloussa H, Migonney V, Falentin-Daudré C (2019) Review of titanium surface modification techniques and coatings for antibacterial applications, Acta Biomat. 83: 37-54

[2] Raut JS and Karuppayil SM (2014) A status review on the medicinal properties of essential oils, Ind. Crops Prod. 62: 250–264.

[3] Di Pasqua R, Betts G, Hoskins N, Edwards M and Ercolini D (2007) Toxicity of Antimicrobial Compounds from Essential Oils, J. Agric. Food Chem 55: 4863–4870.

[4] Nazzaro F, Fratianni F and De Martino L (2013) Effect of Essential Oils on Pathogenic Bacteria, Pharmaceuticals 6: 1451–1474.

[5] Faleiro ML (2011) Chapter: The mode of antibacterial action of essential oils, in Science against microbial pathogens: communicating current research and technological advances, in Science against microbial pathogens: communicating current research and technological advances, Méndez-Vilas (Ed.) 1143–1156.

[6] Swamy MK, Akhtar MS and Sinniah UR (2016) Antimicrobial Properties of Plant Essential Oils against Human Pathogens and Their Mode of Action : An Updated Review Evidence-Based Complement. Altern. Med. 2016: 1–21.

[7] Nagar GB and Pradesh U (2015) In vitro antimicrobial activity , phytochemical analysis and total phenolic content of essential oil from Mentha spicata and Mentha piperita Int. Food Res. J. 22: 2440–2445

[8] Kamatou GPP, Vermaak I, Viljoen AM and Lawrence BM (2013) Menthol : A simple monoterpene with remarkable biological properties, Phytochemistry 96: 15–25

[9] Anghel I, Grumezescu V, Andronescu E, Anghel Ga, Grumezescu Am, Mihaiescu De and Chifiriuc Mc (2012) Protective effect of magnetite nanoparticle / salvia officinalis essential oil hybrid nanobiosystem against fungal colonization on the provox ® voice section prosthesis, Dig. J. Nanomater. Biosctructures 7: 1205–1212.

[10] Magetsari R, Dewo P, Saputro B and Lanodiyu Z (2014) Cinnamon Oil and Chitosan Coating on Orthopaedic Implant Surface for Prevention of Staphylococcus Epidermidis Biofilm Formation, Malaysian Orthop. J. 8: 11–14.

[11] Anghel I, Holban AM, Andronescu E, Grumezescu AM and Chifiriuc MC (2013) Efficient surface functionalization of wound dressings by a phytoactive nanocoating refractory to Candida albicans biofilm development, Biointerphases 8: 1–8.

[12] Zhaveh S, Mohsenifar A, Beiki M, Khalili T S, Abdollahi A, Rahmani-Cherati T, Tabatabaei M (2015) Encapsulation of Cuminum cyminum essential oils in chitosan-caffeic acid nanogel with enhanced antimicrobial activity against Aspergillus flavus, Ind. Crops Prod. 69: 251–256.

[13] Mishra N, Rai VK, Yadav KS, Sinha P, Kanaujia A, Chanda D, Jakhmola A, Saikia D and Yadav NP (2016) Encapsulation of Mentha Oil in Chitosan Polymer Matrix Alleviates Skin Irritation, AAPS Pharm. Sci.Tech. 17: 482–492.

[14] Vega O, Araya JJ, Chavarría M and Castellón E (2016) Antibacterial biocomposite materials based on essential oils embedded in sol–gel hybrid silica matrices, J. Sol-Gel

Sci. Technol. 79: 584–595.

[15] Boumhara K, Tabyaoui M, Jama C and Bentiss F (2015) Artemisia Mesatlantica essential oil as green inhibitor for carbon steel corrosion in 1 M HCl solution : Electrochemical and XPS investigations, J. Ind. Eng. Chem. 29: 146–155.

[16] Diao W, Hu Q, Zhang H and Xu J (2014) Chemical composition , antibacterial activity and mechanism of action of essential oil from seeds of fennel (Foeniculum vulgare Mill .), Food Control 35: 109–116.

[17] Benavides S, Villalobos-Carvajal R and Reyes J E (2012) Physical, mechanical and antibacterial properties of alginate film: Effect of the crosslinking degree and oregano essential oil concentration, J. Food Eng. 110: 232–239.

[18] Sinico C, De Logu A, Lai F, Valenti D, Manconi M, Loy G, Bonsignore L and Fadda AM. (2005) Liposomal incorporation of Artemisia arborescens L. essential oil and in vitro antiviral activity, Eur. J. Pharm. Biopharm.: 161–168,.

[19] Liolios CC, Gortzi O, Lalas S, Tsaknis J and Chinou I (2009) Liposomal incorporation of carvacrol and thymol isolated from the essential oil of Origanum dictamnus L. and in vitro antimicrobial activity, Food Chem. 112: 77–83.

[20] Mossotti R, Ferri A, Innocenti R, Zelenková T, Dotti F, Marchisio DL and Barresi AA (2015), Cotton fabric functionalisation with menthol/PCL micro- and nano-capsules for comfort improvement, J. Microencapsul. 32: 650–660.

[21] Grumezescu AM, Chifiriuc MC, Saviuc C, Grumezescu V, Hristu R, Mihaiescu DE, Stanciu GA and Andronescu E (2012) Hybrid Nanomaterial for Stabilizing the Antibio fi lm Activity of Eugenia carryophyllata Essential Oil, IEEE Trans. Nanobioscience 11: 360–365,.

[22] Ferraris S, Spriano S, Pan G, Venturello A, Bianchi CL, Chiesa R, Faga MG, Maina G and Vernè E (2011) Surface modification of Ti-6Al-4V alloy for biomineralization and specific biological response: Part I, inorganic modification, J. Mater. Sci. Mater. Med. 22: 533–545.

[23] Spriano S, Ferraris S and Vernè E, European Patent 2214732.

[24] Alankar S (2009) A review on peppermint oil, Asian J. Pharm. Clin. Res. 2: 27–33.

[25] Luxbacher T (2014) The zeta potential for solid surface analysis.

[26] ASTM D3359 (2009) Standard Test Methods for Rating Adhesion by Tape Test, Annu. B. ASTM Stand: 1–7.

[27] Banche G, Bracco P, Allizond V, Bistolfi A, Boffano M, Cimino A, Brach del Prever EM and Cuffini AM (2015) Do Crosslinking and Vitamin E Stabilization Influence Microbial Adhesions on UHMWPE-based Biomaterials ?, Clin Orthop Relat Res. 473: 974–986.

[28] Banche G, Bracco P, Bistolfi A, Allizond V, Boffano M, Costa L, Cimino A and Cuffini AM (2011) Vitamin E blended UHMWPE may have the potential to reduce bacterial adhesive ability, J Orthop Res. 29: 1662–1667.

[29] Banche G, Allizond V, Bracco P, Bistolfi A, Boffano M, Cimino A, Brach del Prever EM and Cuffini AM (2014) Interplay between surface properties of standard , vitamin

E blended and oxidised ultra high molecular weight polyethylene used in total joint replacement and adhesion of Staphylococcus aureus and Escherichia coli, Bone Joint J. 96: 497–501.

[30] Ferraris S, Venturello A, Miola M, Cochis A, Rimondini L and Spriano S (2014) Antibacterial and bioactive nanostructured titanium surfaces for bone integration, Appl. Surf. Sci. 311: 279–291.

[31] Ferraris S, Truffa Giachet F, Miola M, Bertone E, Varesano A, Vineis C, Cochis A, Sorrentino R, Rimondini L , Spriano S (2017) Nanogrooves and keratin nano fi bers on titanium surfaces aimed at driving gingival fi broblasts alignment and proliferation without increasing bacterial adhesion, Mater. Sci. Eng. C 76: 1–12.

[32] Ferraris S, Venturello A, Miola M, Cochis A, Rimondini L and Spriano S (2014) Antibacterial and bioactive nanostructured titanium surfaces for bone integration, Appl. Surf. Sci. 311: 279–291.

[33] Legault J and Pichette A (2007) Potentiating effect of β-caryophyllene on anticancer activity of α-humulene, isocaryophyllene and paclitaxel, J. Pharm. Pharmacol. 59: 1643–1647.

[34] Khojasteh-bakht SC, Chen W, Koenigs L. L, Peter RM and Nelson SD (1999) Metabolism of (r)-(+)-pulegone and (r)-(+)-menthofuran by human liver cytochrome p-450s : evidence for formation of a furan epoxide, Drug Metab. Dispos. 27: 574–580.

[35] Kattel R, Devkota and Laxman KC (2015) Fourier Transform Infrared Spectroscopy Analysis of Oil of Menthaarvensis Grown At Sites Varying With Vehicular Traffic Loads in Lucknow City, India, Int. J. Environ. 4: 130–139.

[36] Petrakis EA, Kimbaris AC, Pappas CS, Tarantilis PA, Polissiou MG, Quantitative Determination of Pulegone in Pennyroyal Oil by FT-IR Spectroscopy (2009) J Agric Food Chem. 10044–10048.

[37] Schmitz D, Shubert VA, Betz T and Schnell M (2015) Exploring the conformational landscape of menthol , menthone , and isomenthone : a microwave study, Front. Chem. 3: 1–13.

[38] Maia LF, Fernandes RF, Almeida MR and De Oliveira LFC (2015) Rapid assessment of chemical compounds from Phyllogorgia dilatata using Raman spectroscopy, 25: 619–626.

[39] FT-IR Reference Manual Ed. ABB (2003)

[40] Sandosh TA, Peter MPJ and Raj JY (2013) Phytochemical Analysis of Stylosanthes fruticosa using UV-VIS , FTIR and GC-MS, Res. J. Chem. Sci. 3: 14–23.

[41] Renato Cozzi TR and Protti P (2000), Bande di assorbimento ir, in Elementi di analisi chimica strutturale, Ed. ESU: 2–35.

[42] Moulder JF, Stickle WF, Sobol PE and Bomben KD, Handbook of X-Ray Photoelectron Spectroscopy, edited by J. Chastain (Perkin-Elmer, Eden Prairie, MN, 1992).

[43] Morra M, Cassinelli C, Bruzzone G, Carpi A, Di Santi G, Giardino R and Fini M (2003) Surface Chemistry Effects of Topographic Modification of Titanium Dental Implant Surfaces :1. Surface Analysis, Int. J. Oral Maxillofac. Implant. 41: 40–45,.

[44] Textor M, Sittig C, Frauchiger V, Tosatti S and Brunette DM (2001) Properties and Biological Significance of Natural Oxide Films on Titanium and Its Alloys. In: Titanium in Medicine. Engineering Materials. Springer, Berlin, Heidelberg .

[45] Vincent Crist B (1999) Handbooks of Monochromatic XPS Spectra, ed. XPS International, Inc.

[46] Song HJ, Park SH, Jeong SH and Park YJ (2009) Surface characteristics and bioactivity of oxide films formed by anodic spark oxidation on titanium in different electrolytes, J. Mater. Process. Technol. 209: 864–870.

[47] Neo YP, Swift S, Ray S, Gizdavic-Nikolaidis M, Jin J and Perera C. O.(2013) Evaluation of gallic acid loaded zein sub-micron electrospun fibre mats as novel active packaging materials, Food Chem. 141: 3192–3200.

[48] Zhang X, Ferraris S, Prenesti E and Verné E (2013) Surface functionalization of bioactive glasses with natural molecules of biological significance, part I: Gallic acid as model molecule, Appl. Surf. Sci. 287: 329–340.

[49] Roessler S, Zimmermann R, Scharnweber D, Werner C and Worch H (2002) Characterization of oxide layers on Ti6Al4V and titanium by streaming potential and streaming current measurements, Coll. Surf. B Biointerf. 26: 387–395.

[50] Znini M, Bouklah M, Majidi L, Kharchouf S, Aouniti A, Bouyanzer A, Hammouti B, Costa J and Al-Deyab SS (2011) Chemical Composition and Inhibitory Effect of Mentha Spicata Essential Oil on the Corrosion of Steel in Molar Hydrochloric Acid, Int. J. Electrochem. Sci. 6: 691–704,.

[51] Anghel I and Grumezescu AM (2013) Hybrid nanostructured coating for increased resistance of prosthetic devices to staphylococcal colonization, Nanoscale Res. Lett., 8: 2–7.

[52] Ferraris S, Spriano S, Bianchi CL, Cassinelli C (2011) Surface modification of Ti-6Al-4 V alloy for biomineralization and specific biological response : part II , alkaline phosphatase grafting, J Mater Sci Mater Med. 22: 1835–1842.

[53] Schlaad H (2012) Bio-synthetic polymer conjugates, 253rd ed. Springer.

[54] Ulrey RK; Barksdale SM; Zhou W; van Hoek ML (2014) Cranberry proanthocyanidins have anti-biofilm properties against Pseudomonas aeruginosa, BMC Compl.. Altern. Med. 14: 499.

[55] Savickiene N, Jekabsone A, Raudone L, Abdelgeliel AS, Cochis A, Rimondini L, Makarova E, Grinberga S, Pugovics O, Dambrova M, Pacauskiene IM, Basevičiene N, Viškelis P (2018) Efficacy of Proanthocyanidins from Pelargonium sidoides Root Extract in Reducing P. gingivalis Viability While Preserving Oral Commensal S. salivarius, Materials (Basel) 11: 1499-1514

Table 1: GC-MS analysis of peppermint EO. The % area was corrected removing the contaminants.

Compound	Retention time [min]	Area [%]
cis-Ocimene	4.37	0.27
γ-Terpinene	4.48	0.48
α-Pinene	5.31	0.16
Sabinene	5.45	0.53
δ-3-carene	5.54	0.68
dl-Limonene	6.94	1.00
1,8-Cineol	7.10	5.90
(-)-CIS-2-Carene	8.42	0.39
Camphene	8.46	0.50
Menthone	11.59	15.12
Menthofuran	11.88	15.26
ISO-Menthylacetate	12.34	0.70
-(-)-Menthol	12.70	35.03
-neo-menthol	13.11	0.39
Pulegone	14.91	6.58
Camphane	17.11	6.78
α-Copaene	20.52	0.15
α-Bourbonene	20.82	0.80
Trans-caryophyllene	22.28	3.53
3,7-Guaiadiene	22.70	0.18
δ-Cadinene	23.27	0.13
α-Humulene	23.70	0.16
Bicyclosesquiphellandrene	24.75	1.46
Butyl-methoxy-benzene	25.12	0.74
1- Menthofuranone	25.40	1.59
2- Menthofuranone	26.28	0.21
(-)-Mintlactone	26.57	0.27
(+)-Aromadendrene	29.24	1.01

Table 2: Compounds ~~found~~ detected by GCMS analysis on the biomolecules detached from the samples CT_Mentha oil and CT_50% Mentha oil (soaking). The % area was corrected removing the contaminants.

Samples	**Compound ~~identified~~**	**RT [min]**	**Area [%]**
CT_Mentha oil	Menthol	12.17	44.13
	Hydroxyl-menthofuran	13.53	32.03
	Menthyl-acetate	14.41	4.68
	Beta-cubebene	24.17	19.16
CT_50%Mentha oil (soaking)	Beta-cubebene	24.26	44.86
	Trans-caryophyllene	21.81	55.13

Table 3: Contact angles of the samples Ti6Al4V ~~mirror~~ polished and CT before and after coating/ functionalization.

Samples	Contact angle [deg]
Ti6Al4V ~~mirror~~ polished	77°± 7°
CT	62°± 7°
CT_Mentha oil	77°± 1°
CT_50%Mentha oil (soaking)	99°± 5°

Table 4: FTIR peaks of Mentha piperita EO assignment.

Wavenumber [cm^{-1}]	**Assignment**
3407	O-H stretch [35]
2952 2921 2869	C-H stretching in -CH_3 and CH_2 groups [35]
2721	C-H stretching in aldehydes [35]
1710	C=O stretching vibration [35]
1456 1400 1380 1369	C-H deformation of CH_2 and CH_3 groups [36, 37], primary alcohols O-H bending [35]
1307 1289	CH_3 wagging + twisting + rocking, C-H deformation in the $=C(CH_3)_2$ group [36]
1215 1245 1258 1289	Esters and phenol carbonyl C-O stretching, C-O-C asymmetric stretching in ethers [35]
1079 1095 1100	C-O-C symmetric stretching in ethers[38]
1045 1025	C-O in alicyclic alcohols [36]
991 974 885 875 843	CH_2 and CH out-of-plane deformation vibration in $=CH_2$ and aromatic compounds [38]
763 733 549	Aromatic C-H out-of-plane deformation [36]

Table 5: Atomic percentage of the elements on the surface of the samples CT, CT_ Mentha oil and CT_50%Mentha oil (soaking).

	Samples		
Elements [at %]	**CT**	**CT_Mentha oil**	**CT_50% Mentha oil (soaking)**
C	20.7	86	39.1
O	60.7	13.4	45
N	2.3	0.5	-
Ti	16.2	-	13.8
Al	-	-	1.7
Cl	-	-	0.4

Table 6: main results derived from the z potential titration curves.

Samples	**IEP**	**z (pH=7.4) [mV]**	**Z (pH=6) [mV]**	**Z (pH=8) [mV]**	**Δz Plateau (pH 6-8) [mV]**
CT	<2	-40	-39	-40	-1
CT_Mentha oil	3.1	-70	-54	-76	-22 (no plateau)
CT_50%Mentha oil (soaking)	3.0	-57	-47	-56	-9

Figure captions

Figure 1*: Images of the macroscopic aspect of the samples.*

Figure 2*: Fluorescent microscope images of the samples CT, CT_Mentha oil and CT_50%Mentha oil (soaking).* ~~*Magnification = 20x*~~

Figure 3*: FTIR spectra of A) Mentha piperita liquid EO of Pancalieri (spectrum in absorbance), B) CT samples bare and coated/ functionalized. b1) magnification between 4000-2400 cm^{-1} of the spectra of CT samples bare and coated/ functionalized, b2) magnification between 2400-1000 cm^{-1} of the spectra of CT samples bare and coated/ functionalized.*

Figure 4*: XPS detailed analysis of the oxygen region of the samples a) CT, b) CT_Mentha oil, c) CT_ 50%Mentha oil (soaking).*

Figure 5*: Zeta potential vs pH titration curves of the samples CT, CT_Mentha oil, CT_50%Mentha oil (soaking).*

Figure 6*: a) CT_Mentha oil sample, b) CT_Mentha oil sample after the incision procedure of tape test, c) CT_Mentha oil sample after the tape test (magnification 5x), d) CT_Mentha oil sample after the tape test (magnification 10x).*

Figure 7*: Count of the adherent bacteria (CFU/ml) on the sample surface after 24h of incubation.*

Figure 8*: S. aureus biofilm viability after 24 (a), 48 (b) and 72 (c) hours samples' infection. Cells viability by optical density in function of time (d) and as percentage of bacteria viability in comparison with* ~~*smooth*~~ *polished Ti6Al4V (e). Bars represent means and standard deviations.*

Figure 9*:72 hours S. aureus biofilm Live/dead assay. Magnification = 20x.*

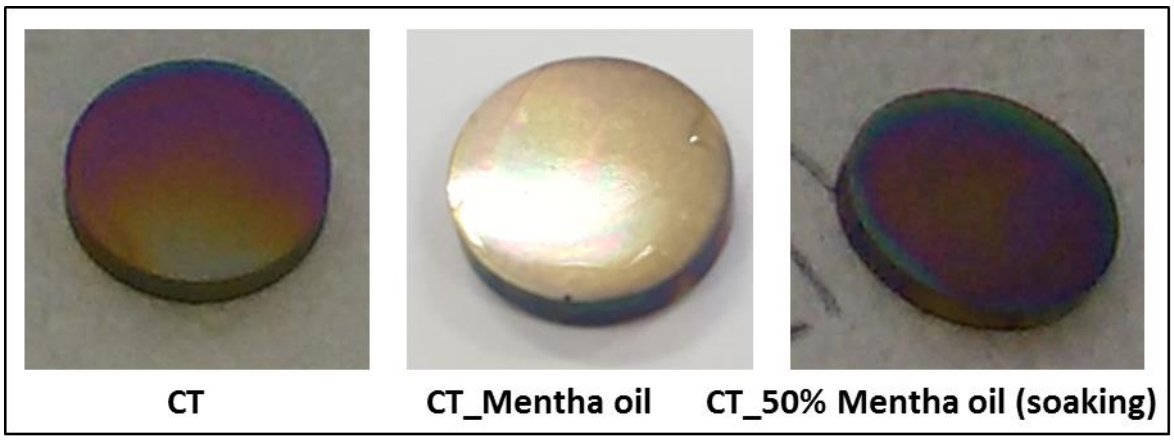
CT
CT_Mentha oil
CT_50% Mentha oil (soaking)

1

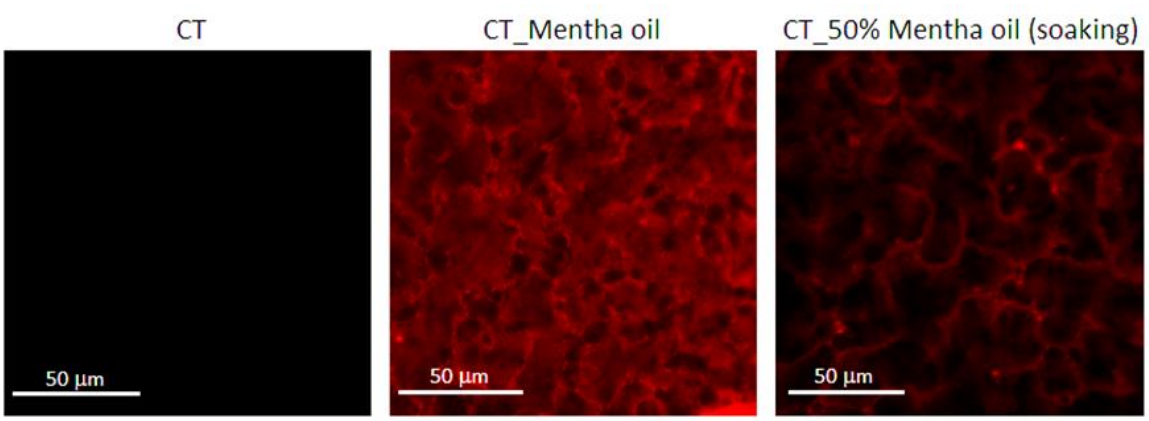
CT
CT_Mentha oil
CT_50% Mentha oil (soaking)
50 µm
50 µm
50 µm

2

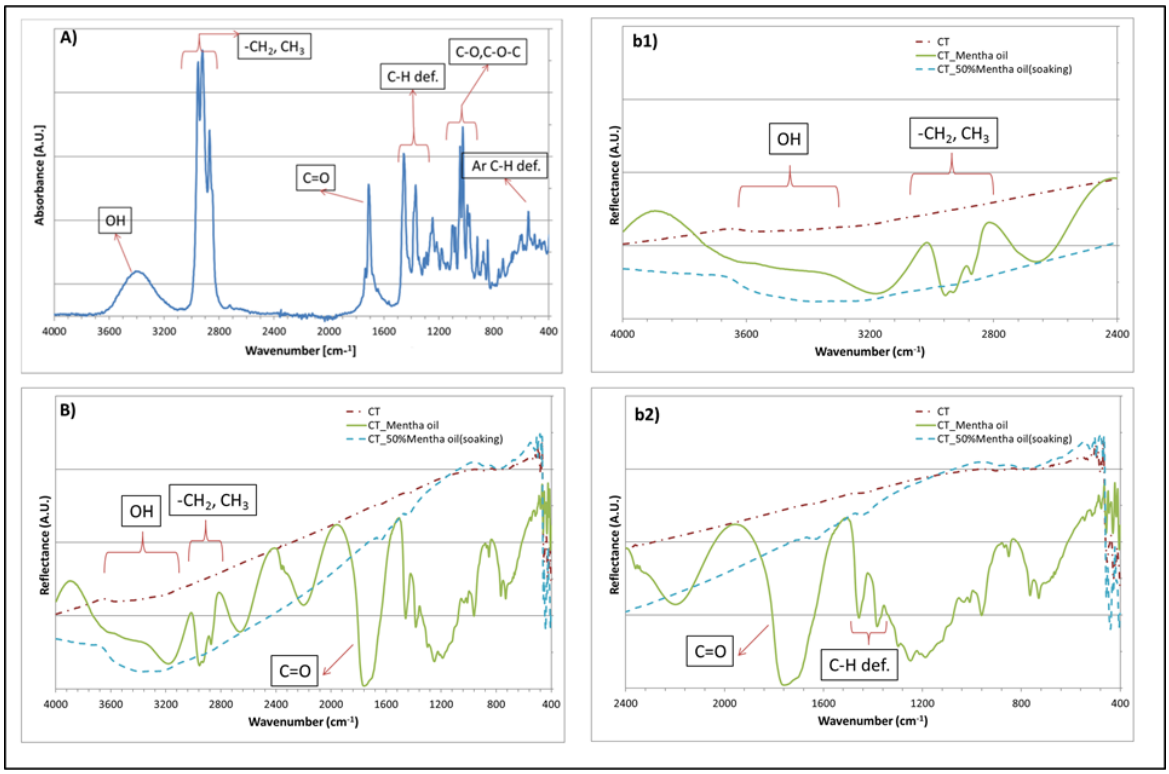
A)
-CH2, CH3
C-O,C-O-C
C-H def.
C=O
Ar C-H def.
OH
Absorbance [A.U.]
Wavenumber [cm-1]
b1)
CT
CT_Mentha oil
CT_50%Mentha oil(soaking)
OH
-CH2, CH3
Reflectance (A.U.)
Wavenumber (cm-1)
B)
OH
-CH2, CH3
C=O
b2)
C=O
C-H def.

3

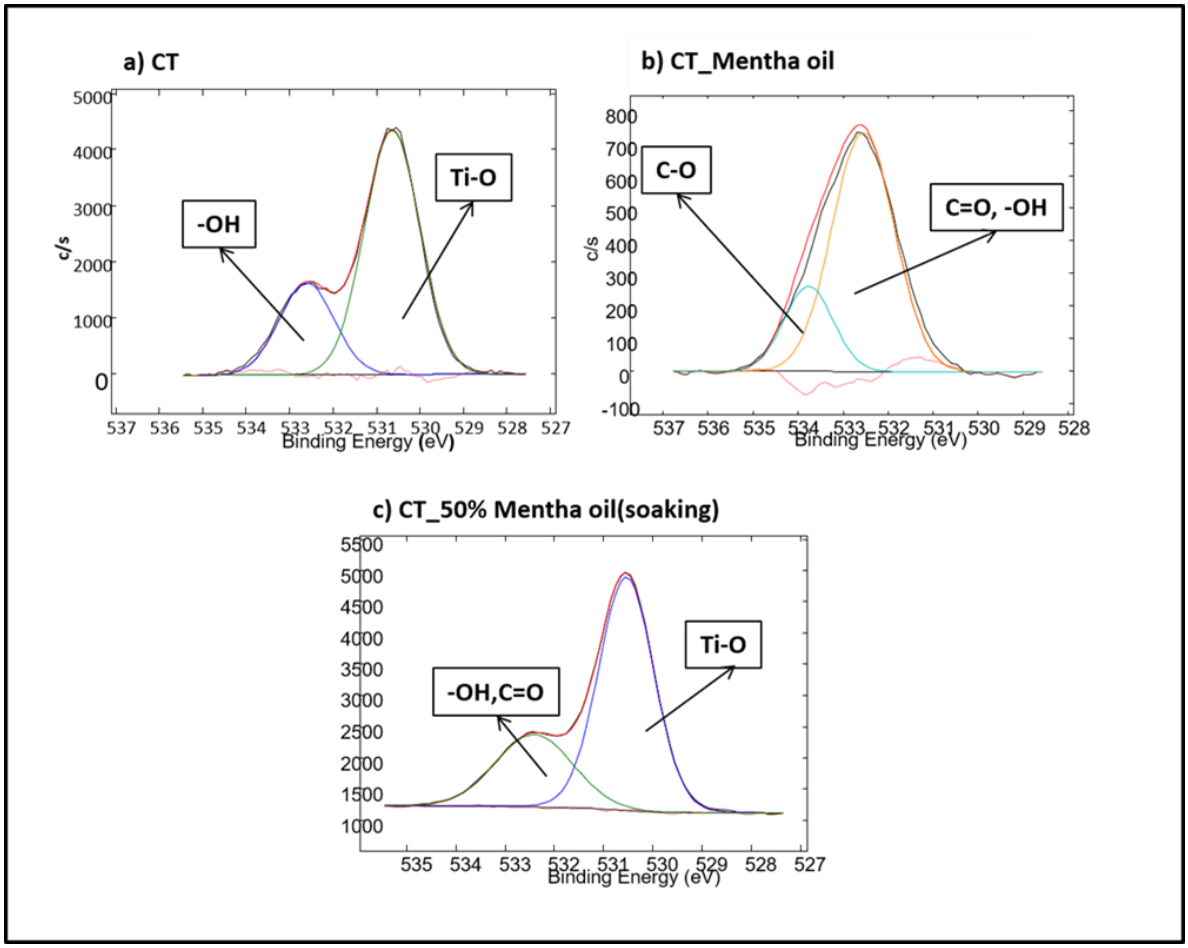
a) CT
-OH
Ti-O
c/s
Binding Energy (eV)
b) CT_Mentha oil
C-O
C=O, -OH
c) CT_50% Mentha oil(soaking)
-OH,C=O
Ti-O

4

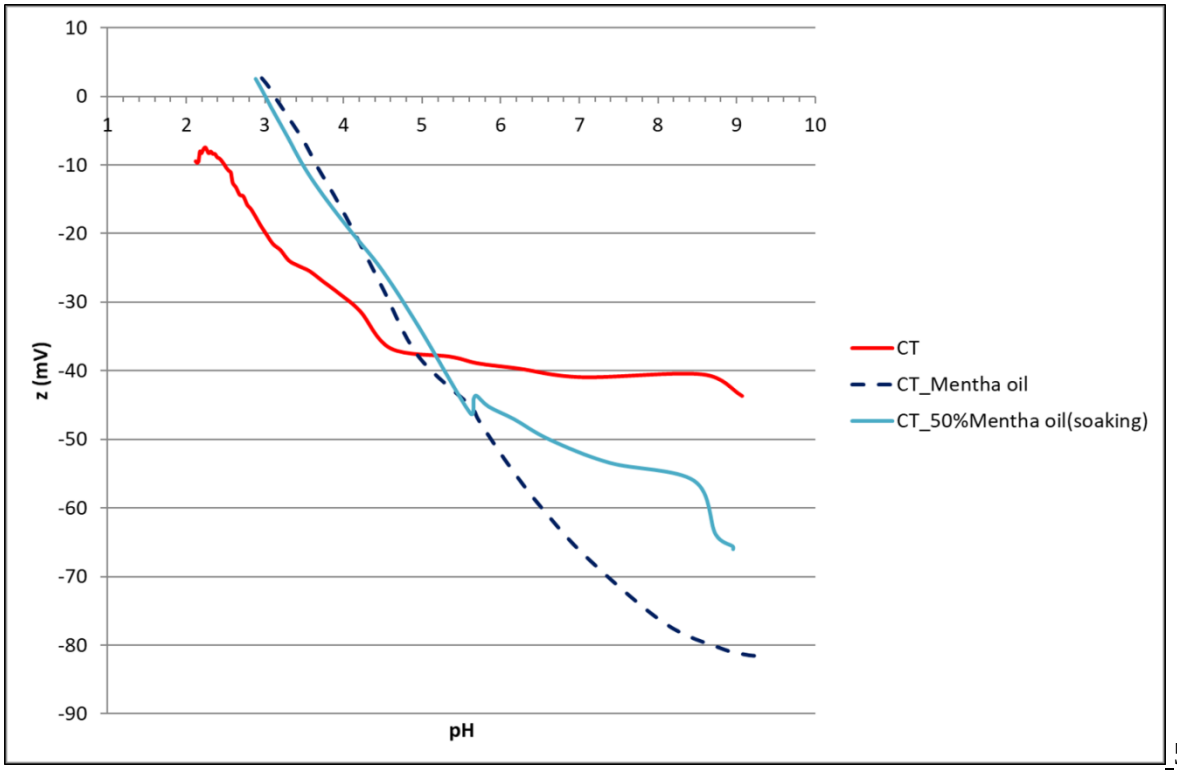
10
0
-10
-20
-30
-40
-50
-60
-70
-80
-90
1
2
3
4
5
6
7
8
9
10
z (mV)
pH
CT
CT_Mentha oil
CT_50%Mentha oil(soaking)

5

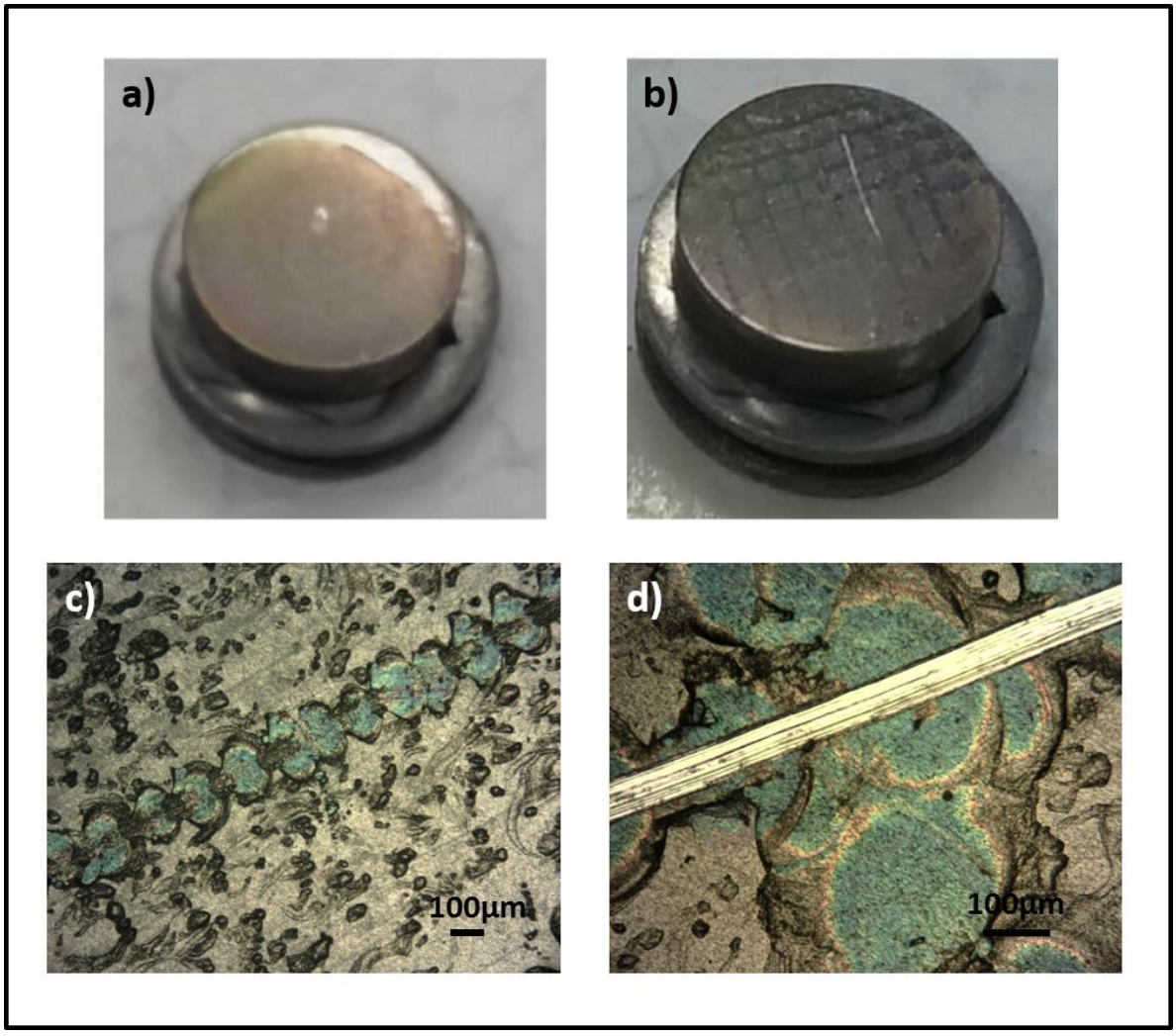
a)
b)
c)
100µm
d)
100µm

6

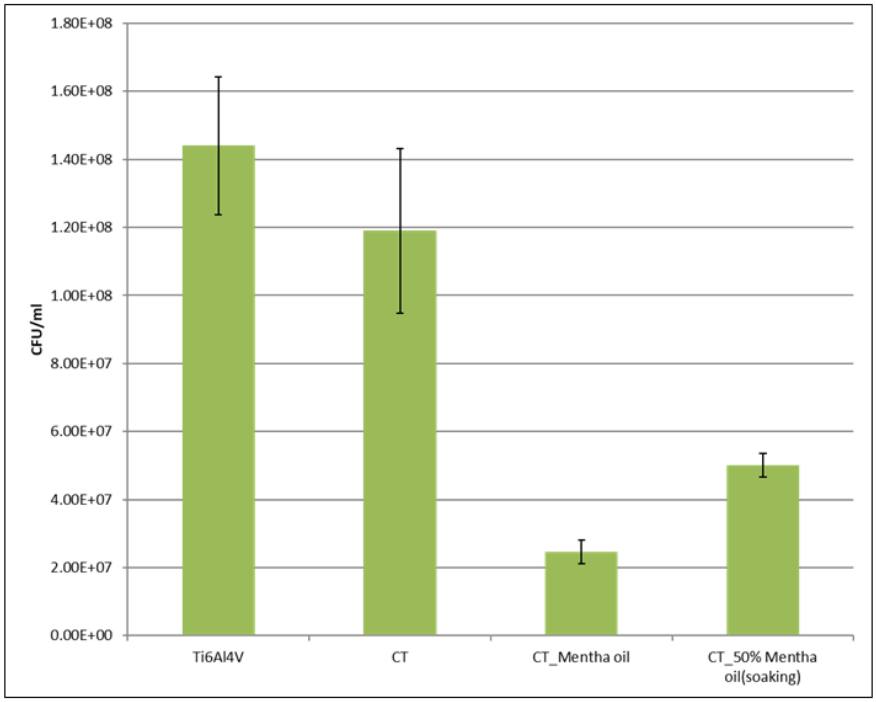
1.80E+08
1.60E+08
1.40E+08
1.20E+08
1.00E+08
8.00E+07
6.00E+07
4.00E+07
2.00E+07
0.00E+00
CFU/ml
Ti6Al4V
CT
CT_Mentha oil
CT_50% Mentha oil(soaking)

7

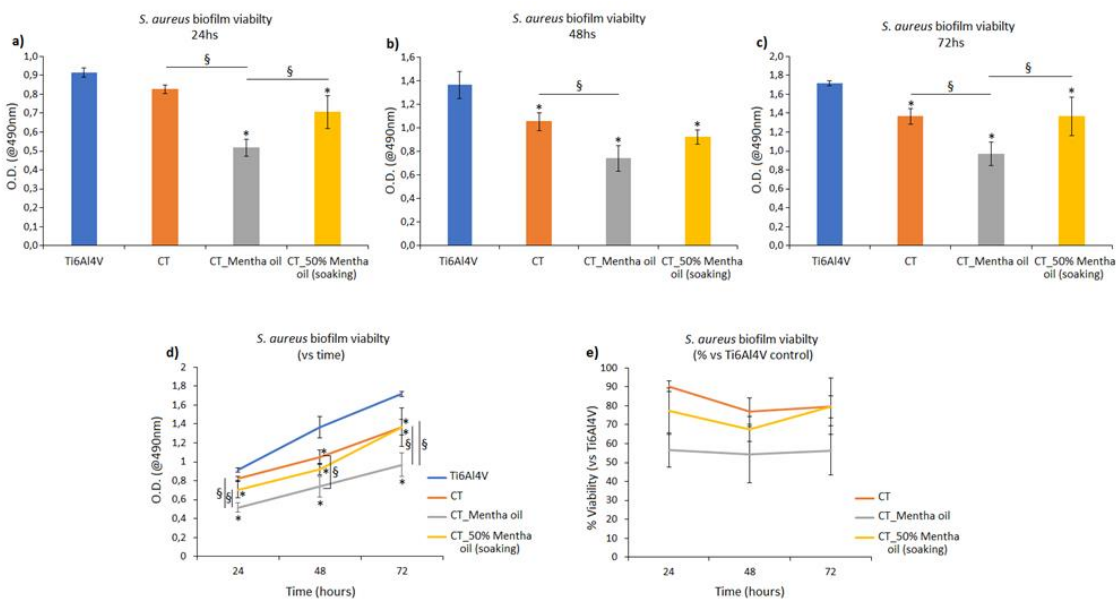
a)
S. aureus biofilm viabilty 24hs
b)
S. aureus biofilm viabilty 48hs
c)
S. aureus biofilm viabilty 72hs
O.D. (@490nm)
Ti6Al4V
CT
CT_Mentha oil
CT_50% Mentha oil (soaking)
d)
S. aureus biofilm viabilty (vs time)
Time (hours)
e)
S. aureus biofilm viabilty (% vs Ti6Al4V control)
% Viability (vs Ti6Al4V)

8

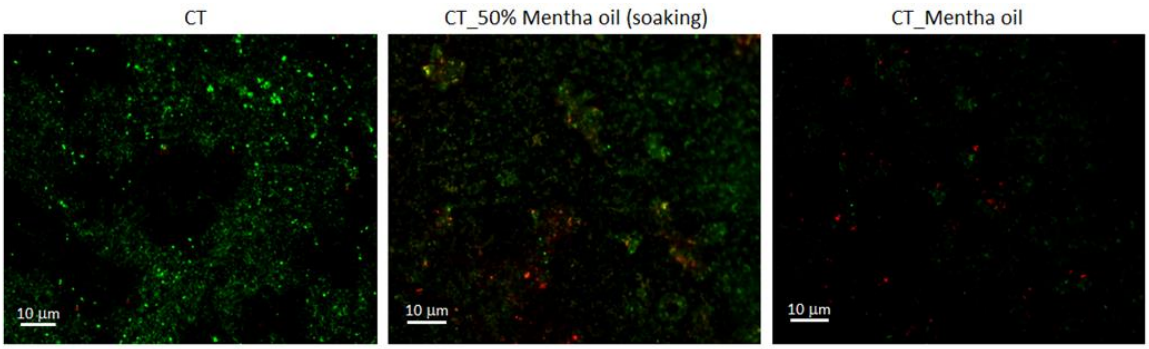

9

Figure1

Click here to download high resolution image

Figure 2 rev

Click here to download high resolution image

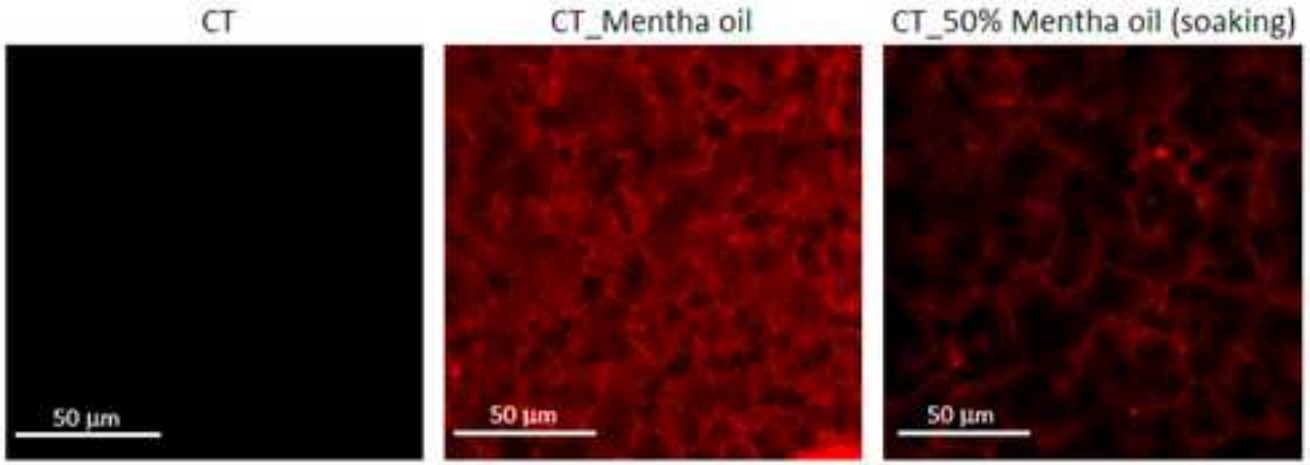

Figure 3 rev

Click here to download high resolution image

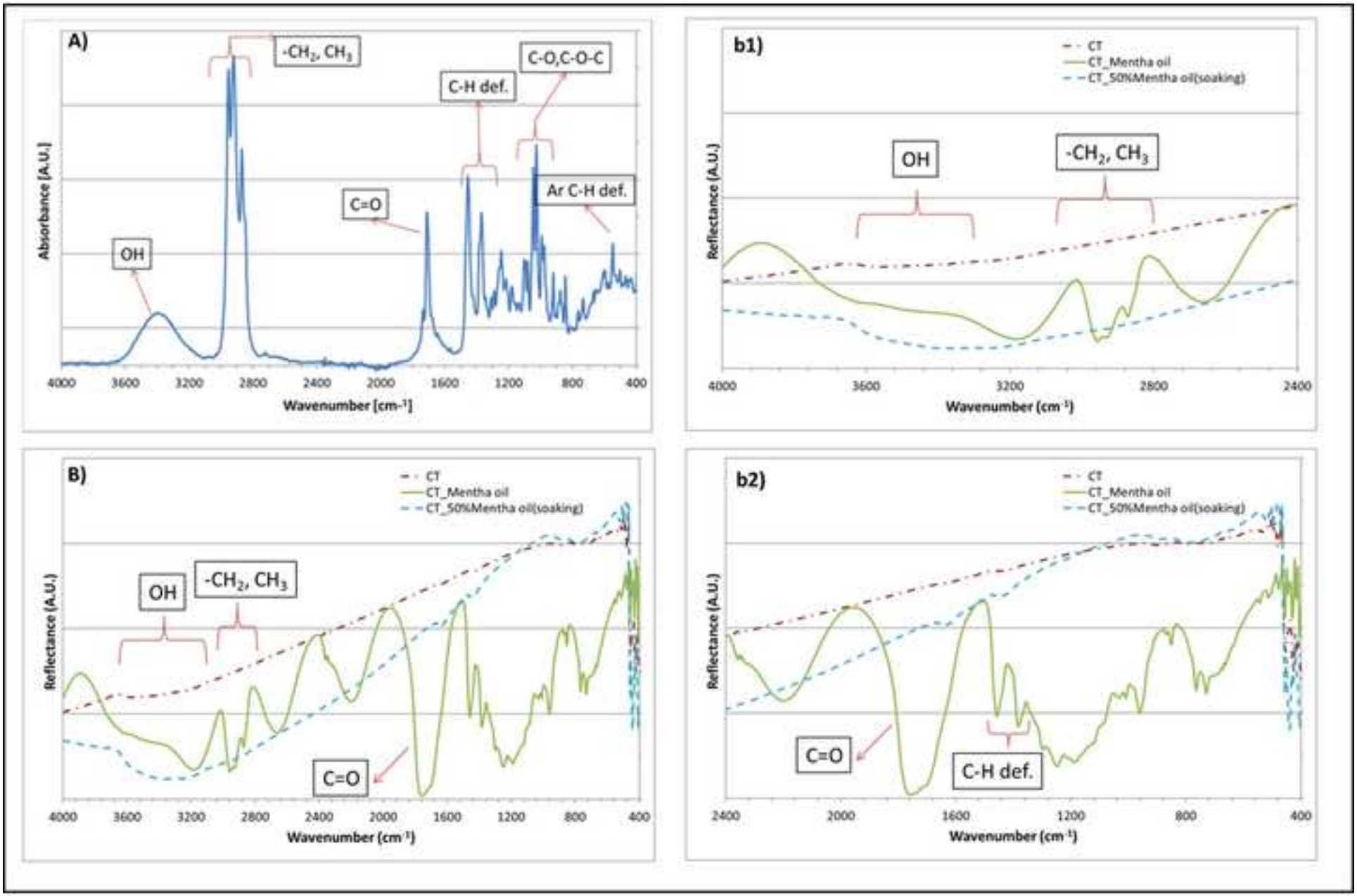

Figure4

Click here to download high resolution image

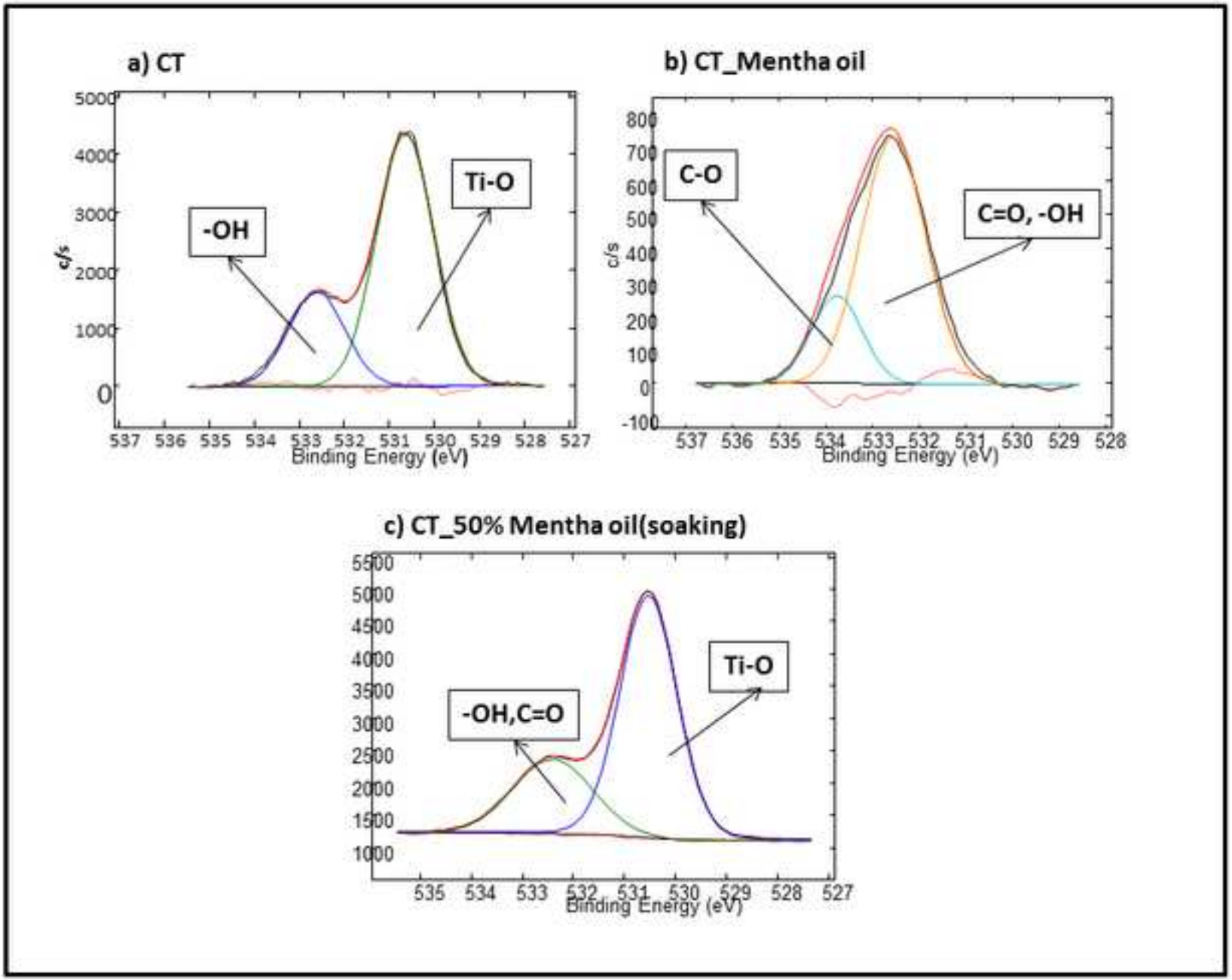

Figure5

Click here to download high resolution image

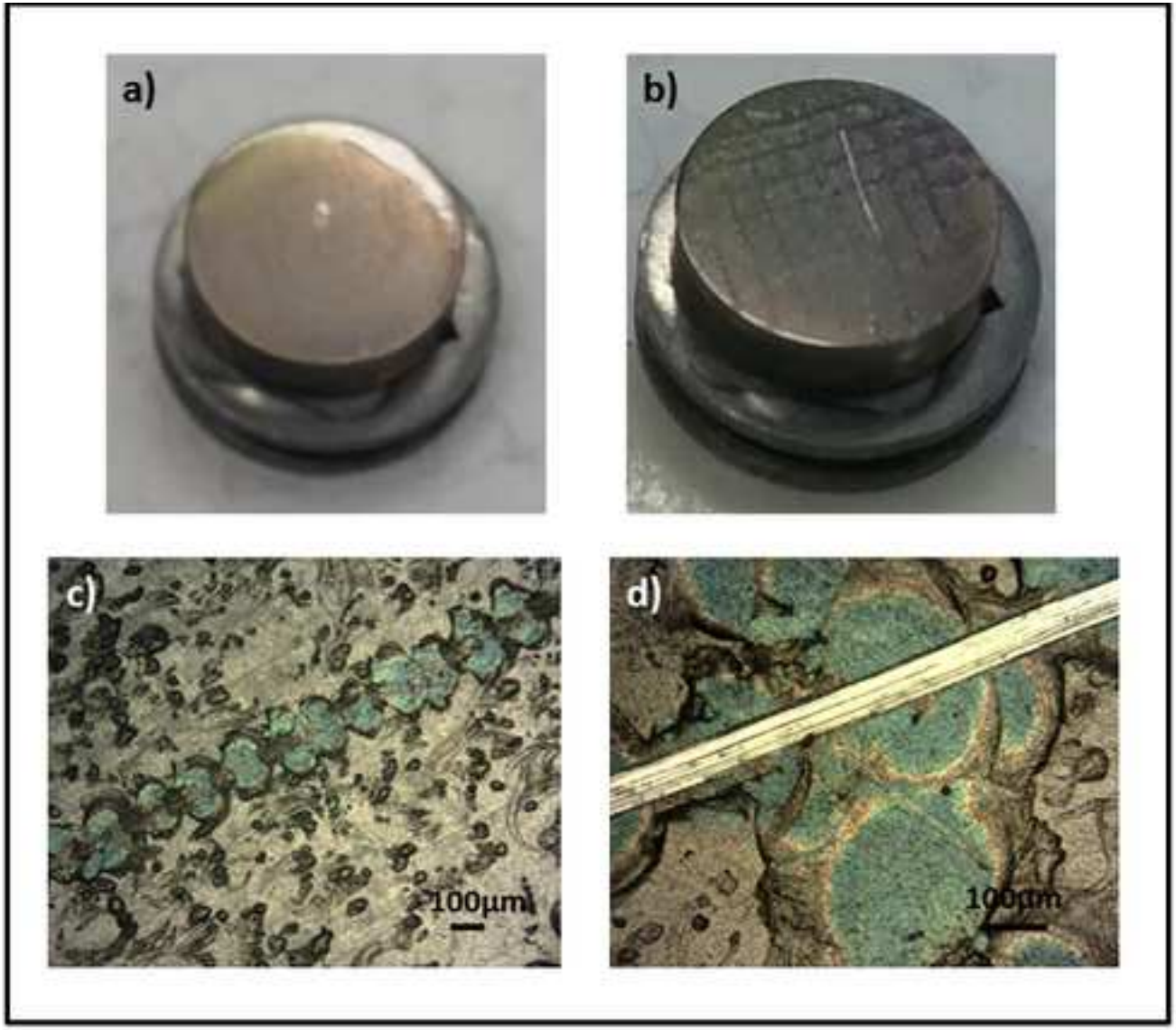

Figure6

Click here to download high resolution image

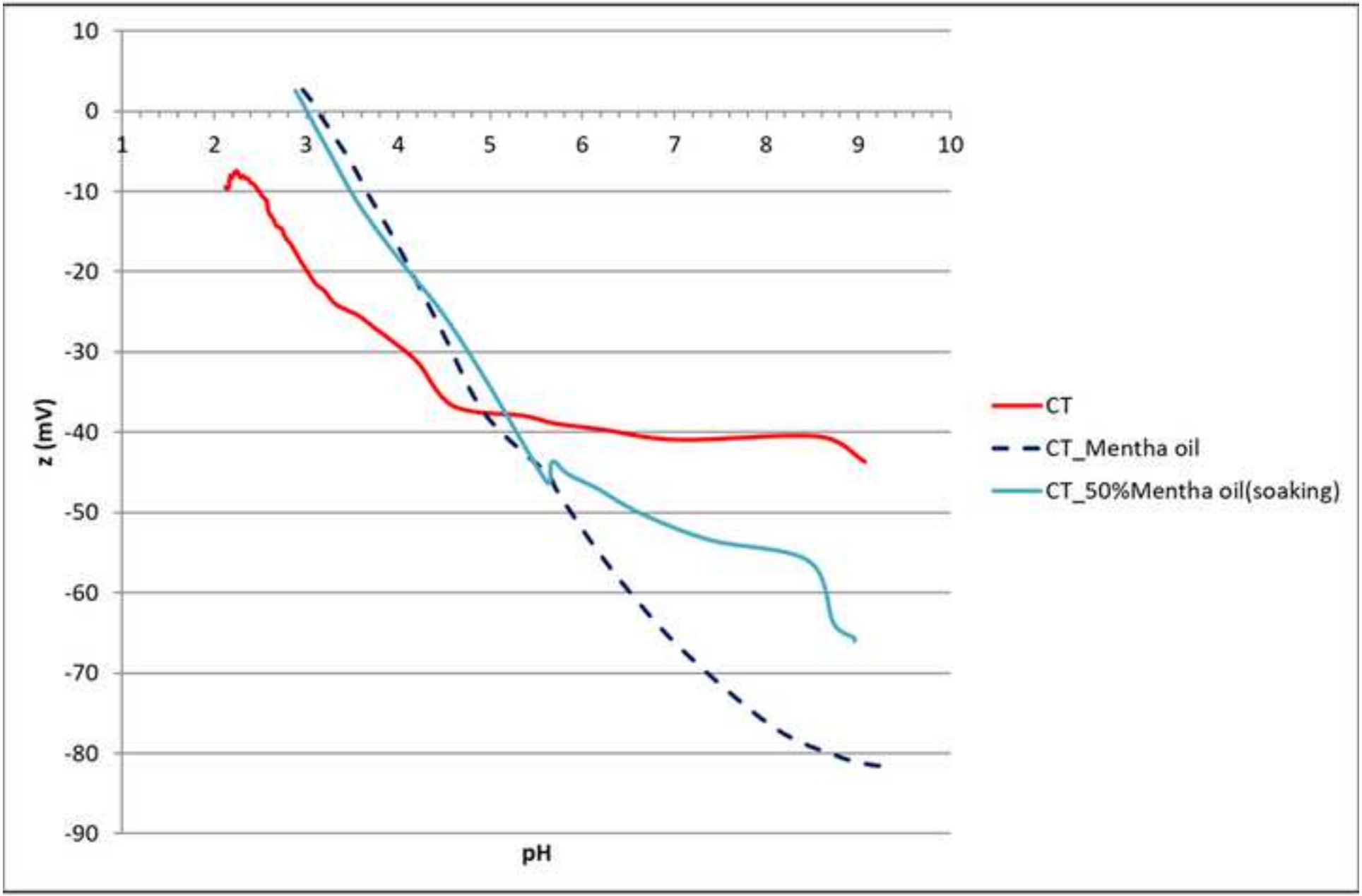

Figure7

Click here to download high resolution image

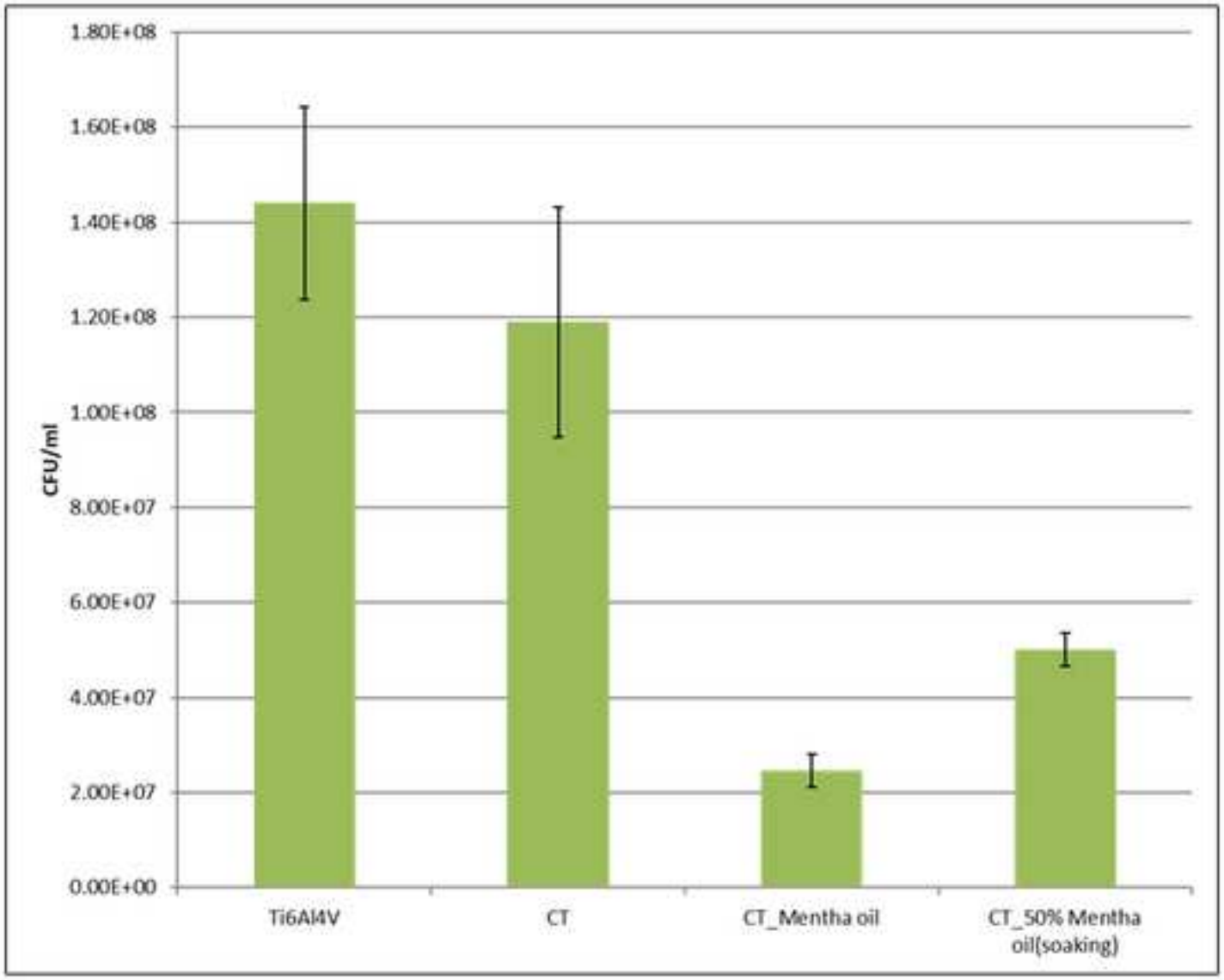

Figure 8 rev

Click here to download high resolution image

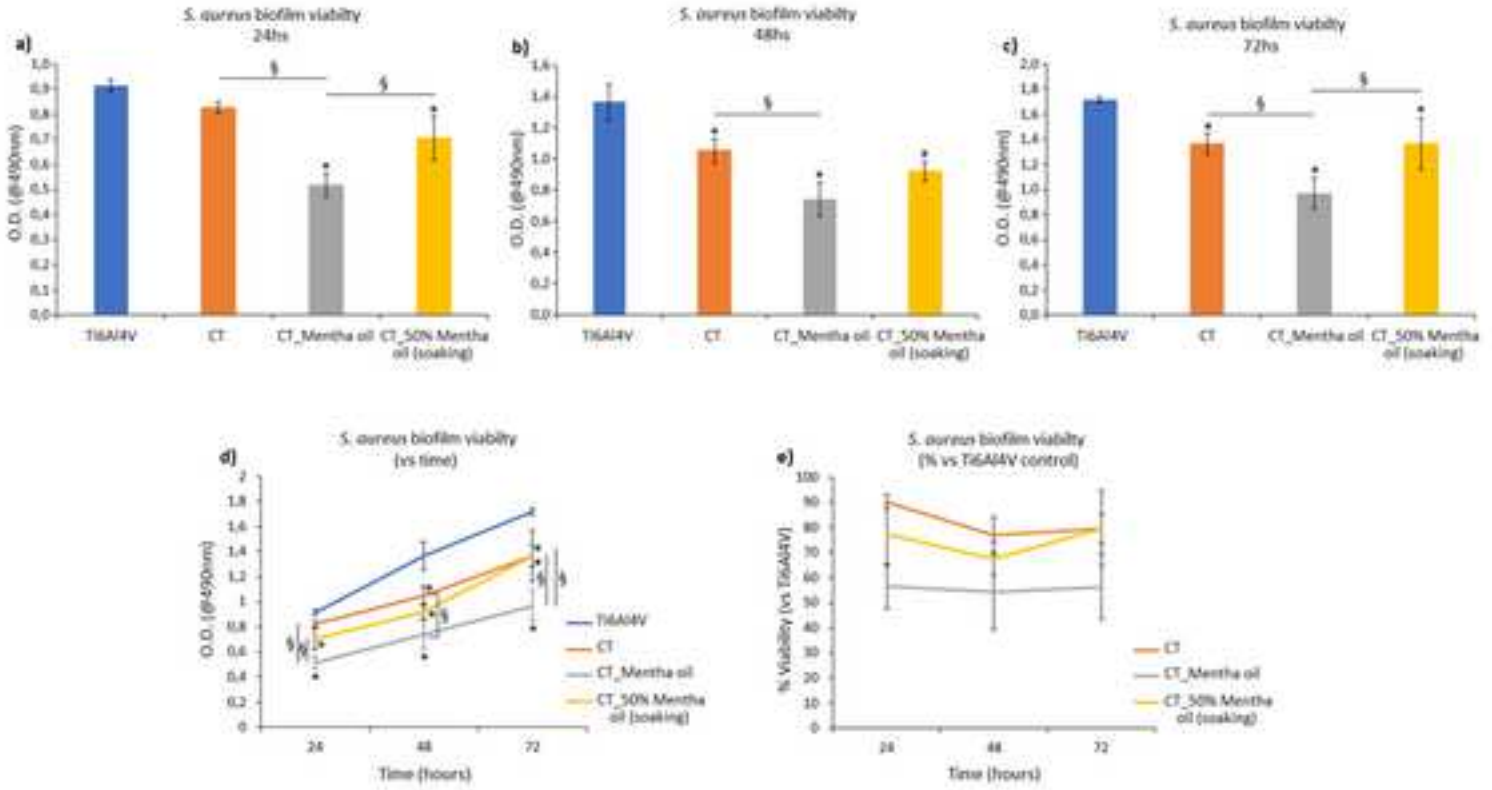

Figure 9 rev

Click here to download high resolution image